Casting lightweight stiff aluminium systems: a review

Sajjad Amirkhanlou, Shouxun Ji*

Brunel Centre for Advanced Solidification Technology (BCAST), Institute of Materials and Manufacturing, Brunel University London, Uxbridge UB8 3PH, United Kingdom

*Corresponding author, Tel: +44-1895-266663; Fax: +44-1895-269758;

Email: shouxun.ji@brunel.ac.uk

Abstract:

Lightweight casting aluminium structural components, in particular shaped castings, are always designed on the criteria of either yield strength or stiffness (Young's modulus). Currently, there are limited options for the aluminium alloys with outstanding Young's modulus compared with conventional aluminium alloys. Moreover, strengthening mechanisms, which result in a significant improvement of the yield strength, may not have a significant effect on the Young's modulus. This review focuses on the Young's modulus of cast aluminium alloys and composites, as well as hybrid materials, with the fabrication processes and microstructure. The effect of different chemical elements in cast alloys, the constituents of in-situ and ex-situ formed aluminium matrix composites and the metallic wire-enhanced hybrid materials on the Young's modulus of aluminium-based materials are reviewed. The Young's modulus of cast aluminium alloys can be improved by: (a) appropriate alloying elements, such as Li, Be, Si and Ni; (b) introducing high modulus reinforcement phases – such as TiB_2, SiC, B_4C and Al_2O_3 – into aluminium by in-situ reactions or by ex-situ additions; and (c) forming hybrid materials with metallic wire reinforcement in the aluminium matrix.

Keywords: Cast aluminium alloys; high modulus materials; metal matrix composites; light metals; stiffness.

1. Introduction

Weight reduction through applying aluminium structural components in aerospace and automobile industries is one of the most promising ways to decrease energy and fuel consumption [1,2]. These structural components, in particular shaped castings, are usually designed on the criteria of either yield strength or stiffness [3,4]. When the yield strength is used as the design criterion, aluminium alloys with much higher strength than pure aluminium are commercially available and these can be selected for industrial applications [5,6]. However, when the stiffness is used as the design criterion, there are limited options for the aluminium alloys with significantly increased stiffness than that of aluminium [7,8]. There is a lack of thorough understanding of the stiffness of aluminium alloys and aluminium-based materials that can be used to make castings. Moreover, some of the strengthening mechanisms, which result in a significant improvement in yield strength, have no obvious effect on the stiffness [9,10]. This has limited the applications of aluminium alloys in the shaped castings and components that require high modulus to achieve further weight reduction in the aluminium structures.

Young's modulus is a measure of the stiffness or rigidity of a solid material or component, which is the resistance to deflection. Pure aluminium has a Young's modulus of 70 GPa. The higher the value of the Young's modulus, the stiffer the material. Young's modulus can be considered as the energy released when two atoms bond together. The simplest description for this energy variation is the Lennard-Jones potential [11], as:

$$U = 4\varepsilon\left[\left(\frac{\theta}{r}\right)^{12} - \left(\frac{\theta}{r}\right)^{6}\right] \qquad (1)$$

where U is the energy, r is the atomic separation, 4ε characterises the depth of the potential well (the bonding energy) and θ is the diameter of the well. If an atom is displaced from its natural position at the lowest energy, then the restoring force is $F = -\,\partial U/\partial r$. Since energy = force × distance, each bond is given by $\partial F/\partial r$, corresponding the gradient of the force line at the position. In the other words, the Young's modulus is the ratio of stress over strain at the initial stage of deformation, showing the bond's property in the material [12,13].

As the intrinsic property of materials, the Young's modulus of cast aluminium alloys can only be marginally influenced by manipulating traditional metallurgical variables that can change the atomic structure of aluminium alloys [14,15]. Chemical composition and phase constituents are two main factors governing the stiffness properties of casting alloys [16]. Processes that can change the microstructure can alter the Young's modulus. The high concentration of alloying elements can have perceptible influence through the contribution in bind interaction. In fact, the high modulus phases can be introduced into the aluminium matrix through alloying elements and/or ceramic particles

[17,18]. The addition of ceramics into the aluminium matrix to form aluminium matrix composites (AMCs) has been the topic of numerous investigations [19,20], in which the high modulus phases can be generated by in-situ reactions with different metallic elements or non-metallic ceramic compounds, or by direct injection of foreign phases. In a similar way, hybrid materials such as wire reinforced metallic structures can be recognised as a special category of composites in macro scale [21], which can be used for an effective increase of Young's modulus. In general, the Young's modulus of cast aluminium alloys is less sensitive to alloying as compared to the stiffer reinforcement in AMCs or hybrid materials.

The methods that have been used to measure Young's modulus are generally described as static methods and dynamic methods. The static methods are carried out through a simple tension (or compression) test or bending test, based on the principle of Hook's law. The Young's modulus is determined by the stress divided by the strain in the linear portion of a plot of stress versus strain. Specific criteria for specimen dimensions and shapes are given in ASTM E8 [22]. Quasistatic tests to evaluate the elastic constants should be carried out according to the procedures outlined in the ASTM E111-04 [23]. Two points are normally noted for the static measurement: one is the difference of Young's modulus determined in tension and compression; and the other is that the tangent modulus or chord modulus are recommended for practical applications, rather than fitting a straight line when the stress-strain curve is not straight in the elastic range. Dynamic methods include the ultrasonic pulse technique [24], the natural frequency vibration method [25], and the free resonance by impulse excitation or continuous excitation [26,27].

There are fundamental reasons for the differences between the dynamic and static techniques. Dynamic methods for measuring the Young's modulus have advantages over the usual static methods [28]. Static tests are considered to be an isothermal process because the slow measurement allows heat dissipation during the test. Ultrasonic tests take place so fast that the conditions are adiabatic and the sample's temperature changes during the test. Similarly, resonant tests are usually adiabatic, depending on the size of the specimen and the resonant frequency. Generally, static tests tend to obtain higher stresses than dynamic tests and so, consequently, the higher-order elastic behaviour is implicitly included in static measurements. Smith et al. [29] identified that the accuracy of the Young's modulus of an Inconel alloy is better than 1% by using the dynamic techniques, but it only achieves an accuracy of 5-7% on the same alloy when the Young's modulus is determined by the static techniques. Although the method of measurement is not covered in the present review, it is necessary to consider this when working on the Young's modulus of materials.

The understanding of the successes and challenges in the stiffness of materials can serve as a guidepost for where future work is needed in order to effectively propel the technology development.

Therefore, this review focuses on the Young's modulus of cast aluminium alloys, composites and hybrid materials and their fabrication processes, aiming to provide a snapshot of the current progress on cast aluminium alloys for improving their Young's modulus. The paper is outlined as follows. Section Two summarises the effect of alloying elements of Li, Be, Si, Cu, Ni, Cr and Mg on the microstructure and Young's modulus of aluminium alloys. Section Three focuses on the stiffness improvement by in-situ and ex-situ composites. A discussion on the processing, microstructure and Young's modulus of the in-situ and ex-situ reinforcement – including TiB_2, TiC, AlN, ZrB_2 and Al_2O_3 – in cast Al alloys is provided. The properties of commonly used reinforcements are discussed in association with the merits and limitations of processing. Section Four summarises the effect of wire reinforcement on the Young's modulus of aluminium hybrid materials. Section Five ends the paper with the summary and future outlook.

2. Effect of alloying elements

The effect of alloying elements on the stiffness property of aluminium alloys depends on whether they are present in solutions or in second phases. When the alloying elements are present in solid solutions, the elastic constant is determined by the nature of atomic interactions and the interatomic potentials [30,31]. In particular, the atomic size differences and the electronic structure determine the Young's modulus of solid solution aluminium alloys. There are two methods to define the atomic size factor: one is defined as $(\Omega_S^* - \Omega_{Al})/\Omega_{Al}$, where Ω_{Al} is the mean atomic volume of the aluminium atom and Ω_S^* is the effective volume of the solute atom, as calculated from lattice parameter data [32,33]; the other is defined as $(\Omega_S^* - \Omega_S)/\Omega_S$ for aluminium-based alloys, where Ω_S is the true atomic volume of the solute atom [33,34]. The later parameter can be a direct measure of the deviation from Vegard's Law [35], which can predict the linear dependence of atomic volume on the concentration between the values for pure solvent and pure solute. Deviation from the law in a metallic solid solution reflects the change of electronic environment around the atoms, which further influences the bonding properties and hence the Young's modulus.

Figure 1 shows the change in the Young's modulus of solid solution alloys plotted as a function of both atomic size factors. Mg has a very large volume size factor (+40% in Figure 1a) but shows only a small deviation from Vegard's Law (Figure 1b). The change in the Young's modulus caused by Mg additions is also very small, indicating the importance of electronic effects on modulus rather than strain energy effects. Similarly, for Al-Li alloys, the volume size factor is very small (-2%), but the deviation from Vegard's Law is high, resulting in the high Young's modulus. Therefore, the Young's modulus of a solid solution alloy is probably dependent on a complex combination of several factors. Overall, a high solid solubility of elements is necessary to form a stiff atomic structure in aluminium alloys.

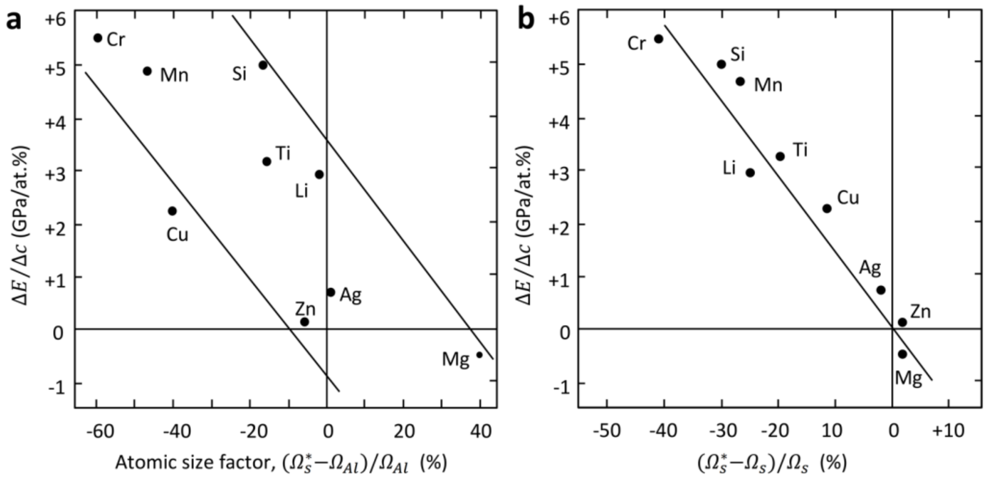

Figure 1. Change in modulus of solid solution alloys plotted as a function of (a) atomic size factor and (b) deviation from Vegard's Law [36].

When the alloying elements are present as second phases, the elastic constant is determined by the volume fraction and the intrinsic modulus of the second phases. The nature of the second phase is important. When the second phases are not coherent with the matrix, the overall modulus is lower than that predicted by the analytical models. Table 1 shows the Young's modulus of various intermetallic phases that are commonly formed in aluminium-based alloys. The Young's modulus of these intermetallic phases is 95-215 GPa, which is higher than the modulus of pure aluminium. The addition of these intermetallic phases can improve the modulus of Al-based alloys. However, the improvement is significantly affected by the type and the amount of intermetallic. For example, 40 vol.% of Al_3Ti is needed to achieve the Young's modulus of 90 GPa in aluminium alloys, but only approximately 20 vol.% of Al_3Ni is possibly enough for obtaining the same level of Young's modulus.

Table 1. Young's modulus of intermetallic phases in aluminium-based systems [37,38,39].

Compound	Young's modulus (GPa)	Compound	Young's modulus (GPa)
AlLi	105	Mg_2Si	120
Al_3Li	95	$AlNi_3$	200
Al_2Cu	105	α-AlFeSi	166
Al_7Cr	130	β-AlFeSi	180
Al_6Mn	125	$Al_{63}Cu_{25}Fe_{12}$	182
Al_3Fe	130	Al_7Cu_2Fe	168
Al_3Ti	150	Al_7Cu_4Ni	163
Al_3Ni	215	$Al_3Cu_2Ni_2$	185

The contents of alloying elements increase the concentration of solute solution strengthening and promote the formation of intermetallic. The Young's modulus and density of aluminium alloys are directly dependent on the contents of each solute element. The dependence can be estimated by summing the percentages of each element multiplied by their own density and/or modulus, respectively (i.e., the rule of averages). As summarised in Table 2, the density and Young's modulus of common elements can be used to estimate the modulus of aluminium-based materials. The trend of the effect of alloying contents on the modulus of aluminium alloys is presented in Figure 2 for the common elements, in which Li, Mn, Be, Ni, Si and Cu increase, but Ca and Mg decrease the Young's modulus of aluminium alloys.

Table 2. Density and Young's modulus of commonly used elements in aluminium alloys [15].

Alloying element	Density ρ (g/cm^3)	Young's modulus E (GPa)
Al	2.70	69
Cr	7.19	248
Cu	8.96	128
Fe	7.87	208
Mg	1.74	44
Mn	7.43	200
Ni	8.90	207
Si	2.33	110
Sn	7.30	44
Ti	4.54	120
Zn	7.13	69
Zr	6.50	49
Li	0.53	4.9
Be	1.85	303

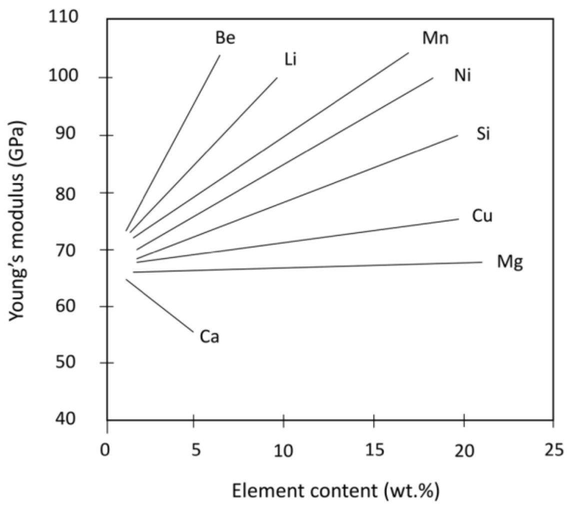

Figure 2. Effect of alloying elements on the Young's modulus of aluminium alloys.

2.1 Lithium (Li)

Lithium is the lightest alloying element in aluminium alloys. The addition of Li into aluminium not only reduces the weight but also increases the Young's modulus of aluminium alloys [36,40]. Every 1 wt.% Li addition reduces the density approximately 3% and increases the Young's modulus approximately 6%, in addition to the contribution to enhance the tensile strength and improve the high cycle fatigue [41,42]. These synergistic property combinations lead to significant increases in specific strength (strength/density) and specific stiffness (E/ρ), as illustrated in Table 3. The E/ρ ratio increases by approximately 10% for the addition of every 1 wt.% Li [43].

Table 3. Specific stiffness obtained from Al-Li alloys with respect to equivalent conventional aluminium alloys [44].

Alloy families	Specific stiffness GPa/(g/cm^3)	Specific buckling resistance (GPa)$^{1/3}$/(g/cm^3)	Improvements in Al-Li alloys	
			Specific Stiffness	Specific Buckling Resistance
2xxx	26.1-27.1	1.48-1.52	+13%	+8%
7xxx	25.9-26.4	1.46-1.50	+15%	+9.5%
3rd-gen. Al-Li alloys*	28.9-31.2	1.58-1.65	-	-

*The first generation Al-Li alloys developed in the late 1950s contain approximately 2 wt.% Li. The second-generation Al-Li alloys developed in the 1970s contain approximately 2 wt.% Li and other elements. Li content was reduced in the third-generation Al-Li alloys to reduce the anisotropic mechanical properties, low short-transverse ductility and fracture toughness.

Figure 3 shows the experimental results for the Young's modulus of Al-Li alloys obtained from different references [36,40]. Noble et al. [36,45] reported that the Young's modulus of both solutionised and aged binary Al-Li alloys increases rapidly over the first few weight percent additions of Li, but the rate of increase drops thereafter. The Young's modulus increases from 77 GPa at 1 wt.% Li to 82-85 GPa at 4 wt.% Li, but further to 94 GPa at 11 wt.% Li. In Figure 3, the results also show that the Young's modulus increases linearly from 73.5 GPa for 2024 alloy to 91 GPa for 2024+4 wt.% Li. The dependence of Young's modulus of 2024 alloy on the amount of lithium can be estimated by: $E_{2024+Li}(GPa) = 4.4\,Li(\%) + 73.5$.

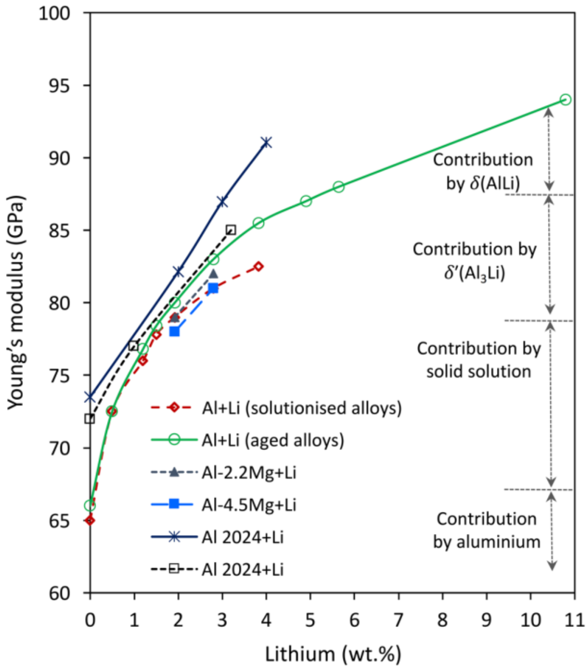

Figure 3. The relationship between the Young's modulus of aluminium alloys and the lithium content [36,40].

The variation of Young's modulus can be interpreted by the microstructure and phase formation. The binary Al-Li alloys consist of α(Al-Li) solid solution, δ'(Al$_3$Li) metastable ordered precipitates and δ(AlLi) equilibrium intermetallic phase [46,47]. After ageing, the metastable δ'(Al$_3$Li) phase is in the form of spheroidal particles, with an ordered L12 structure [48,49]. The sizes of δ' precipitates are 50-200 nm and the volume fractions of δ' precipitates are 1-30% [50,51]. The Young's modulus of δ' phase and δ is at a level of 95 GPa and 105 GPa, respectively [33,36]. It was initially reported that the origin of high modulus for Al-Li alloys is the formation of coherent δ'(Al_3Li) precipitates during ageing [52]. However, the modulus of Al-Li alloys with a quenched single phase of α(Al-Li) solid solution is close to that of the aged alloys with solid solution and δ'(Al_3Li) dual phases [36]. Similarly, Samuel and Champier [53] found that the Young's modulus in Al-2.5%Li alloy under solutionised conditions is almost the same to that under aged conditions. Therefore, the major contribution to the modulus improvement in Al-Li alloys is likely associated with the Al(Li) solid solution. The nearest neighbour (n-n) distance is 0.3031 nm in pure lithium and 0.286 nm in Al-Li solid solution. So the valence electrons in Al-Li alloys are contained in a much smaller volume than that in pure elements. Consequently, the valence electron density in Al-Li solid solutions is higher than that in pure metals, in which the lithium atoms has suffered no reduction in n-n distance. This increases the value of charge density and force constant in Al-Li solid solutions. The high value of the force constant means that the Debye temperature and thus the specific modulus of Al-Li alloys increase with increasing the lithium contents. Therefore, as Al and Li in α(Al-Li) solid solution have very small differences in atomic radius, the appropriate electronic structure can be formed to improve the modulus, as reported by Noble et al. [36] and Fox et al. [54].

In Al-Li alloys, the main additional elements are Cu, Mg, Ag, Zr, Sc, Mn and Zn to activate strengthening mechanisms by a combination of grain refinement and precipitation [41]. The typical composition and Young's modulus of selected Al-Li alloys are summarised in Figure 4. In Al-Li-X alloys, Zr is always added from 0.10 to 0.12 wt.%. Zr affects the course of crystallisation and the grain refinement; it also facilitates the nucleation of δ' phase. The Al_3Zr precipitates also contribute to the homogenisation of dislocation structure. Cu and Mg create additional precipitates in the boundary areas, which reduces the adverse tendency for the occurrence of precipitate-free zones [55]. Adding Mg to Al-Li alloys causes an extra increase of the material's strength, but Mg in Al-Li alloys reduces the Young's modulus [36], in which the reduction is approximately 0.5% when adding 1 at.% Mg. Typical microstructural features in Al-Li-X alloys are schematically shown in Figure 4. On top of the precipitates of T_1(Al_2CuLi) and δ'(Al_3Li) to increase the strength, there are dispersoids such as Al_3Zr and $Al_{20}Cu_2Mn_3$ intermetallic particles, which are mainly compounds of Al with Fe, Mn, Si, Cu and sometimes Mg. When Li is less than 1.4-1.5 wt.%, the T_1(Al_2CuLi) phase is favoured by the presence of Cu and small amounts of Mg and Ag. The S(Al_2CuMg) phase is formed only in the alloys with relatively low Cu content and reasonable additions (~0.8%) of Mg. The non-sharable θ'(Al_2Cu) phase is found in the alloys with low Li content (<0.6%). The β'(Al_3Zr), δ(AlLi), T_2(Al_6CuLi_3) and Al-Fe phases are also found in the alloys with appropriate compositions. In general, there is still a lack of systematic studies for understanding the effect of additional elements on the Young's modulus of Al-Li alloys. However, as the intrinsic modulus of second phases and the volume fraction of precipitates in Al-Li alloys are relatively low, the minor addition of Mg, Ag, Zr, Sc, Mn and Zn elements is expected to have an insignificant effect on the modulus improvement.

Table 4. Compositions and Young's modulus of typical Al-Li alloys [56,57].

Al-Li alloys	Li	Cu	Mg	Ag	Zr	Sc	Mn	Zn	Young's modulus (GPa)
2020	1.2	4.5					0.50		77.0
1420	2.1		5.2		0.11				75.0
1421	2.1		5.2		0.11	0.17			78.0
2090	2.1	2.7			0.11				76.0
2091	2.0	2.0	1.3		0.11				75.0
8090	2.4	1.2	0.8		0.11	0.17			77.0
2195	1.0	4.0	0.4	0.40	0.11				78.6
2297	1.4	2.8	≤0.25		0.11		0.30	≤0.5	77.2
2397	1.4	2.8	≤0.25		0.11		0.30	0.10	
2098	1.0	3.5	0.53	0.43	0.11		≤0.35	0.35	79.0
2198	1.0	3.2	0.5	0.40	0.11		≤0.5	≤0.35	76.7
2099	1.8	2.7	0.3		0.09		0.30	0.70	79.3
2199	1.6	2.6	0.2		0.09		0.30	0.60	78.0
2050	1.0	3.6	0.4	0.40	0.11		0.35	≤0.25	77.9
2296	1.6	2.4	0.6	0.43	0.11		0.28	≤0.25	77.3
2055	1.0	3.6	0.4	0.40	0.11		0.35	≤0.25	78.5
2060	0.7	3.9	0.8	0.25	0.11		0.30	0.40	77.2

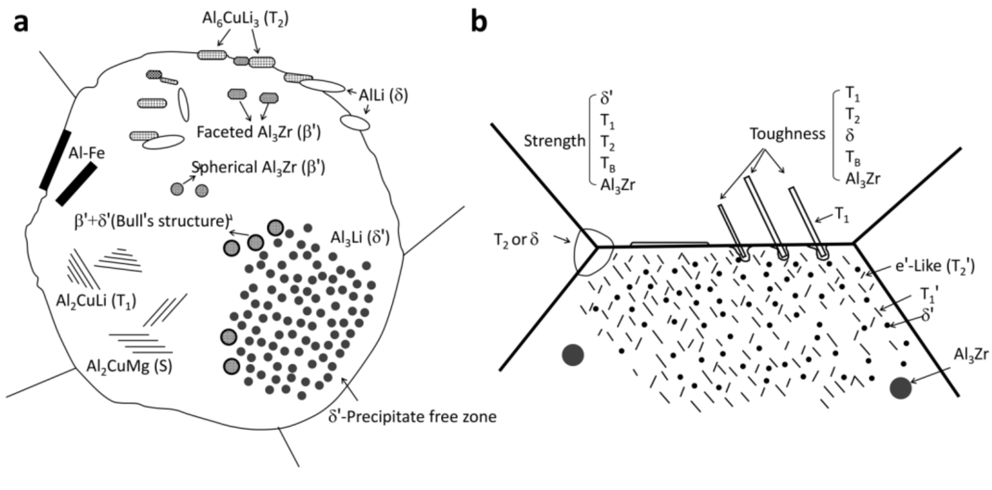

Figure 4. Schematics of typical microstructural features in (a) second- and (b) third-generation Al-Li alloys [58].

2.2 Beryllium (Be)

Beryllium and lithium are the only two elements that can simultaneously reduce the density and increase the Young's modulus of aluminium alloys. In addition to the advantages in structural performance, Be has the thermal conductivity of 210 W/mK and the heat capacity of 1,925 J/kgK. These render Al-Be alloys as excellent materials for thermal management [59]. According to the equilibrium phase diagram [60], Al and Be form a eutectic at a composition of 2.5% Al and a temperature of 644 ºC. The solid solution shows highly limited solubility of Be in Al and no solubility of Al in Be [61]. This gives rise to the potential to treat Al-Be alloys as composite materials and the Young's modulus of the alloys can thus be approximately estimated by the volumetric rule of mixture calculations [62]. The distribution of Be phase in Al matrix depends on the relative quantities of Be and the method used for processing.

The Al-38 wt.% Be alloy can provide the Young's modulus of 195 GPa, as well as 5-7% of elongation and 350 MPa of ultimate tensile strength (UTS) [63]. This alloy has a typical eutectic composition and the microstructure is characterised by fine dispersions of Be phase in Al matrix. Grensing et al. [64] studied the aluminium alloys with Be from 1 to 99 wt.% by investment casting. As shown in Table 5, the Young's modulus of the Al-Be alloys is significantly improved by increasing the Be contents. For example, an increment of 5 wt.% Be produces a 23% higher Young's modulus and 26% greater of specific stiffness. Marder and Haws [65] also obtained similar results after studying semi-solid metal processing of three Al-Be alloys including A356-30% Be, 7075-30% Be, and 7075-30% Be.

Table 5. Stiffness-based properties of Al-Be binary alloys [64,65].

Al-xBe (wt.%)	Density (gr/cm^3)	Specific stiffness (GPa/g/cm^3)	Young's modulus (GPa)	Young's modulus ratio to pure Al
0	2.68	25.69	69	1
5	2.63	32.33	85	1.232
10	2.57	39.23	101	1.464
15	2.52	46.45	117	1.696
20	2.46	53.58	132	1.913
25	2.41	60.21	145	2.101
30	2.38	66.79	159	2.304
35	2.32	73.97	172	2.493
40	2.27	81.51	185	2.681
45	2.24	87.42	196	2.841
50	2.19	95.12	208	3.014
62	2.10	110.76	233	3.377
70	2.05	122.05	250	3.623
80	1.96	136.88	269	3.899
90	1.91	150.27	287	4.159
100	1.85	163.38	303	4.391

Several trials have been carried out for the improvement of Young's modulus of Al-Be alloys. Figure 5 shows the experimental results of Young's modulus obtained from different works for Al-Be alloys [64,65,66,67]. Obviously, the Young's modulus of Al-Be alloys increases almost linearly with the Be contents. Nieh et al. [68] reported the stiffness of a series of Al-Be alloys produced by a rapid solidification technique, which forms a finely dispersed Be phase in the microstructure. Al6061 and Al1100 alloys reinforced with 20 and 40 wt.% Be were studied by Hashiguch et al. [66] via vacuum induction melting and a static casting process. The Young's modulus of cast Al6061-20 wt.% Be and Al6061-40 wt.% Be alloys are 130 and 195 GPa, respectively. The stiffness of Al-Be alloys results from the very low atomic number of Be atoms. As the Be ion is so small and highly polarising to the content, its compounds are rather covalent. When Be forms a metallic phase, the bonds are highly energised and the atoms are tightly bound. Therefore, it requires more energy and larger forces to break Be-based bonds.

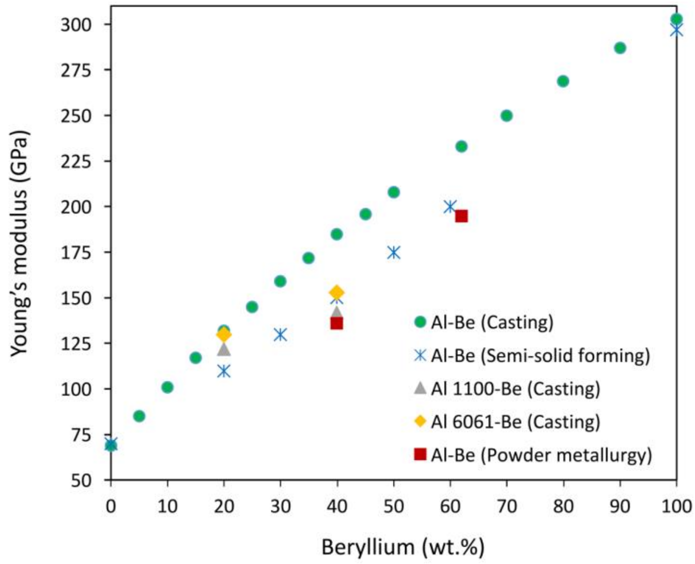

Figure 5. Young's modulus of different aluminium alloys with beryllium [64,65,66,67].

The addition of other elements to Al-Be alloys was reported by Crooks et al. [69] and Jones et al. [70,71,72]. In general, major elements including Si, Cu and Mg and minor elements including Ni, Ti and Sr are typically added to Al-Be alloys to provide strengthening for the Al matrix. The compositions and stiffness-based properties of typical Al-Be alloys are shown in Table 6. The major contribution to the final stiffness-based properties is attributed to the Be and Si elements, while other elements have a minor effect on the Young's modulus. Ochiai et al. [73] reported that the Al-Be-Si-based alloys not only have excellent plastic workability, ductility and strength, as comparable to those of the conventional Al-Si-based alloys, but also possess the specific stiffness and Young's modulus comparable to those of the conventional Al-Be alloys.

The addition of Mg was found to increase the strength of the Al-40 wt.% Be-3 wt.% Mg alloy with almost the same ductility. Fridlyander [59] investigated the microstructure and mechanical properties of Al-Be-Mg alloys and found that the microstructure is composed of a primary crystallising Be phase and a hardened Al solid solution of magnesium in aluminium when Al-Be-Mg systems are in the double-phase range. However, the coarse and segregated $\beta_{Al-Be-Mg}$ phase is presented in the microstructure when the composition of Al-Be-Mg alloys is at the outside of the double-phase region. The mechanical properties are noticeably worsened due to the appearance of the brittle β phase. In comparison with the Al-Li-Mg system, in which Mg usually reduces the Young's modulus, Mg in Al-

Be alloys can increase the Young's modulus [59]. The Young's modulus of Al-Be-Mg alloys is 15-30 GPa higher than that of Al-Be alloys, although the magnesium has a Young's modulus of 45 GPa. However, Crooks et al. [69] reported that Mg can increase the strength by 65% and decrease the Young's modulus by 10% when 8.6 wt.% Mg is added to Al-43 wt.% Be alloy.

The theoretical prediction of Young's modulus has been carried out in several studies. Hashiguchi et al. [66] compared the modulus predicted by the theoretical models with the experimental results and found that the density and Young's modulus of Al-Be-based alloys follow the rule of mixtures, i.e., interpolation of alloy properties is generally possible between the respective properties of pure Be and pure Al. Al-Be alloys have not been widely industrialised because of the cost, difficulties associated with the alloys production and the serious health concerns related to the Be element [74]. It is also difficult to cast Al-Be-based alloys because of the requirement for a vacuum environment. However, the specific stiffness and the capability of lightweight of Al-Be-based alloys offer great potential for structural applications.

Table 6. Compositions and Young's modulus of typical Al-Be alloys [73,75,76].

Be	Si	Mg	Cu	Ni	Co	Fe	Ti	Li	Ag	Sr	Al	Density (g/cm^3)	Specific stiffness ($GPa/g/cm^3$)	Young's modulus (GPa)
4.6	5.9	0.4									Bal.	2.59	27.4	71.0
8.1	6.0	0.4	5.2								Bal.	2.55	31.0	79.1
13.4	5.6	0.5	5.2								Bal.	2.49	37.3	92.7
14.7	9.2	1.4		0.7							Bal.	2.47	37.2	92.0
19.8	8.8	1.6	0.8	0.7							Bal.	2.42	40.9	99.0
20.4	15.3	1.4	0.8	0.8							Bal.	2.45	40.8	100.0
19.7	8.6	1.1	0.8	0.7	1.00						Bal.	2.49	38.9	97.0
20.2	8.8	1.4	0.8	0.8	1.00						Bal.	2.49	40.2	100.0
19.2	8.6	2.3	2.1	0.7	1.00						Bal.	2.49	40.2	100.0
20.1	8.7	1.7	0.8	0.7		0.50					Bal.	2.47	39.3	97.0
24.1	8.9	1.3					0.40				Bal.	2.46	43.5	107.0
20.2	0.14	1.8									Bal.	2.44	40.4	98.5
19.5	0.35	1.0	0.80	0.70	1.00	1.02					Bal.	2.49	39.8	99.0
21.9	0.17	1.52	1.95	0.93	1.04	1.06	0.09				Bal.	2.55	38.5	98.1
20.0	0.14	1.66	1.85	1.45		0.99					Bal.	2.51	39.6	99.3
20.0							0.28	2.4			Bal.	2.29	53.8	123.0
30.0							0.35	1.3			Bal.			142.0
65.0	2.0								2.0	0.04	Bal.	2.10	108.3	227.5
63.0	2.0		0.25						2.0	0.04	Bal.	2.13	106.8	227.5
65.0	2.0				0.25				2.0	0.04	Bal.	2.14	105.3	225.4
65.0	1.0								2.0		Bal.	2.13	112.6	239.9

2.3 Silicon (Si)

Aluminium-silicon (Al-Si) alloys are the most popular cast aluminium alloys because of their excellent combination of castability and mechanical properties [77,78]. In the equilibrium phase diagram of Al-Si alloys [79], silicon can substitute aluminium atoms to form α-Al(Si) solid solution between 0 and 1.65 wt.% Si. A typical hypoeutectic microstructure of the primary α-Al and eutectic α-Al/β-Si phases is formed from 1.65 to 12.6 wt.% Si in the alloys during solidification. Hypereutectic Al-Si alloys with Si>12.6 wt.% show the primary α-Si particles and eutectic α-Al/β-Si phases, whereas the microstructure of eutectic alloy at 12.6 wt.% Si is fully covered with eutectic α-Al/β-Si phase. Figure 6 shows the typical microstructure of Al-Si alloys under as-cast conditions.

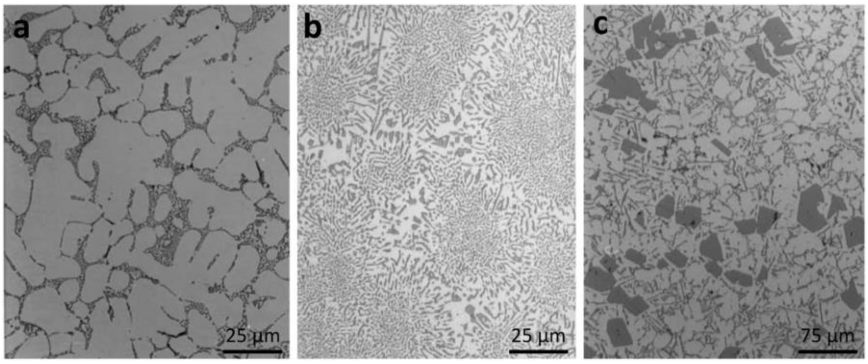

Figure 6. Typical microstructure of as-cast Al-Si alloys: (a) hypoeutectic alloys with 1.65-12.6 wt.% Si, (b) eutectic alloy with 12.6% Si and (c) hypereutectic alloys with >12.6% Si [80].

The stiffness of cast Al-Si alloys depends strongly on the silicon contents and its morphology, which are controlled by solidification and chemical composition. The Young's modulus of Si phase is 160 GPa [81]. As the covalent bonds of silicon atoms are stronger than the metallic bonds of aluminium, the increase of Si content can form more covalent bonds of silicon atoms in Al-Si alloys. Therefore, silicon leads to increases of the Young's modulus in the as-cast alloys. Figure 7 demonstrates the Young's modulus experimentally measured binary Al-Si alloys under as-cast (AC) and heat-treated (ST) conditions at both room and high temperature (RT and HT, respectively). For the hypoeutectic alloys, when the Si contents are increased from 7 to 12 wt.%, the Young's modulus increases from 73 to 77 GPa under as-cast condition. When further increasing the Si contents to 18 wt.%, the hypereutectic Al-Si alloy has a Young's modulus of 84 GPa. This corresponds to the amount of α-Al/β-Si eutectic phases, which is increased from 8% to 13.6% and further to 20.2 vol.% when the Si level is at the level of 7, 12 and 18 wt.%, respectively. In Figure 7, it is also clear that the increase in temperature results in a decrease of Young's modulus in the binary Al-Si alloys. The Young's modulus of 84 GPa at room temperature is decreased to 71 GPa at 300ºC for the Al-18 wt.% Si alloy.

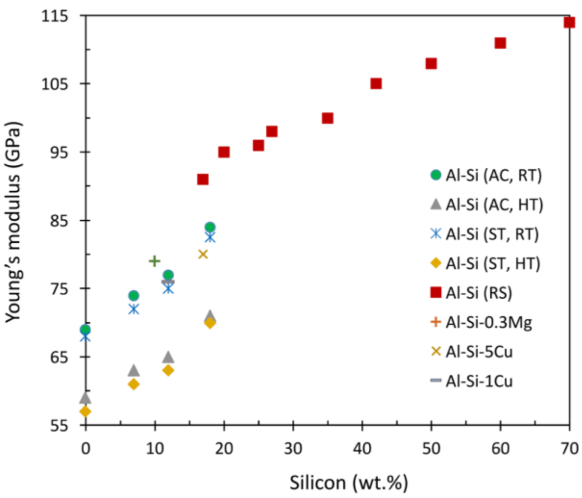

Figure 7. Variation of Young's modulus of aluminium alloys with increasing silicon [81].

Solutionisation of Al-Si alloys can slightly decrease the Young's modulus. Lasagni et al. [81] reported ~2% reduction in the Young's modulus of Al-Si alloys after solution treatment. This is attributed to the morphological modification of the β-Si phase to increase its discontinuity by solution treatment. Generally, the interconnected lamellar Si structure increases the Young's modulus up to the upper boundary predicted by mixture models, while the isolated and spheroidised Si particles obtained by heat treatment are well described by the lower boundary predicted by the mixture models for Al-Si alloys.

The addition of other elements in Al-Si alloys can affect their Young's modulus. For the commonly used Mg, Cu, Mg, Ti, Ni, Mn and Zn [82,83], the chemical compositions and stiffness-based properties are shown in Table 7. The major contribution to the stiffness-based properties is Si and Cu elements, and the other elements have a minor effect on the Young's modulus. The types, size and distribution of intermetallic phases formed in the Al-Si-based alloys alter their Young's modulus because the Young's modulus of the common intermetallic phases β-Mg_2Si, θ-Al_2Cu, S-Al_2CuMg, Al_3Fe and α-AlFeSi is 120, 110, 135, 130 and 166 GPa, respectively [84]. Therefore, the existence of these phases can increase the Young's modulus of Al-Si alloys. However, these elements are added at relatively low levels and the volume fraction of intermetallic phase is low, resulting in an insignificant increase of Young's modulus in Al-Si alloys. Jeong [85] investigated the Young's modulus of Al-12 wt.% Si alloys with different levels of Cu and the results are shown in Figure 8. The typical microstructure of the Al-Si-Cu alloy consists of α-Al, β-Si and Al_2Cu intermetallic phases. The increase of 5 wt.% Cu results in an increase of the Young's modulus, as much as 5 GPa at the given temperatures, compared to Al-12Si alloy. However, the Young's modulus decreases almost linearly with the temperature increases. This is because the increased temperatures weaken the interatomic bonding.

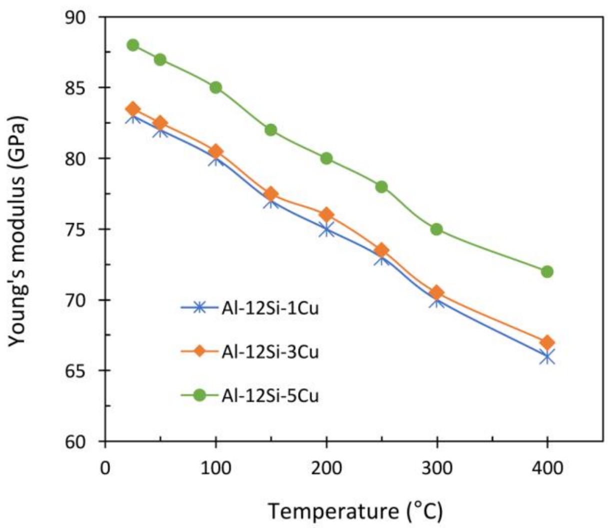

Figure 8. Young's modulus of Al-12Si alloys with different levels of Cu versus temperature [85].

Table 7. Compositions and Young’s modulus of typical Al-Si alloys [86].

Si	Mg	Cu	Mn	Fe	Ti	Zn	Ni	Sn	Al	Density (g/cm^3)	Specific stiffness ($GPa/g/cm^3$)	Young’s modulus (GPa)
2	0.5	0.1	0.3	0.6		0.1		0.04	Bal.	2.70	25.9	70
2		1		0.1					Bal.	2.72	26.1	71
4	1.0		0.1					0.05	Bal.	2.70	26.3	71
5	0.5	3		0.12		0.1	0.04		Bal.	2.71	26.6	72
5	0.1	3.3	0.4	0.8	0.2	0.5	0.30	0.05	Bal.	2.70	26.7	72
6	0.3	4	0.3	0.1	0.15	2.0	0.30	0.04	Bal.	2.71	26.9	73
7	0.3	0.15	0.5	0.5	0.1	0.1			Bal.	2.70	27.4	74
7	0.3	0.1	0.1	0.2	0.1	0.1	0.05	0.03	Bal.	2.70	27.4	74
7	0.57	0.1	0.1	0.2	0.15	0.1			Bal.	2.71	27.5	74.4
7	0.4	3.3	0.4	0.8	0.25	0.5	0.30	0.04	Bal.	2.70	27.4	74
7	0.48	0.95		0.1	0.2		0.02		Bal.	2.72	28.1	76.4
8	0.3	0.1	0.08	0.27	0.09	0.5	0.04		Bal.	2.70	28.1	76
9	0.4	0.01	0.03	0.15	0.1	0.5		0.04	Bal.	2.71	27.7	75
9	0.2	3.2	0.6	1	0.2	1.2	0.50	0.03	Bal.	2.71	28.2	76.4
9	0.02	0.02	0.15	0.3	0.09	0.09	0.04		Bal.	2.65	28.7	76
9.5	0.35	0.02	0.04	0.04	0.12	0.04	0.02	0.05	Bal.	2.72	27.9	76
9.8	0.35	0.04	0.15	0.32	0.12	0.09	0.04	0.03	Bal.	2.65	28.3	75
10	0.3	0.1	0.5	0.6	0.2	0.1	0.05	0.05	Bal.	2.72	27.9	76
10	0.4	0.2	0.27	0.6	0.2	0.2	0.10	0.02	Bal.	2.67	28.7	76
11	0.02	0.02	0.04	0.21	0.09	0.04	0.02		Bal.	2.72	27.9	76
11	0.18	0.02	0.04	0.14	0.1		0.02	0.05	Bal.	2.68	28.4	76
11	0.3	4.8	0.3	0.21	0.2	0.02			Bal.	2.65	28.7	76
12.2	0.1	0.1	0.5	1.2	0.2	0.15	0.10	0.05	Bal.	2.72	27.9	76
12.3	1.3	1.3	0.09	0.55	0.09	0.04	0.90		Bal.	2.65	28.7	76
12.5	0.04	0.01	0.18	0.28	0.14	0.09	0.04	0.05	Bal.	2.72	27.9	76
13	0.1	0.1	0.50	0.7	0.15			0.04	Bal.	2.65	28.8	76.4
13	0.1	0.1	0.2	0.65	0.15		0.05	0.05	Bal.	2.65	28.7	76
17	0.5	4.5	0.1	0.4	0.2	0.05		0.03	Bal.	2.72	29.8	81
17	0.5	4.5	0.5	1.1	0.2	1.5	0.10		Bal.	2.70	30.4	82
17	0.57	4.5	0.1	0.4	0.2	0.04	0.10	0.02	Bal.	2.71	30.3	82
18	1.1	1.2	0.2	0.7	0.2	0.2	0.10		Bal.	2.70	30.4	82
19	1	0.8	0.4	0.1	0.2	0.1	0.10	0.03	Bal.	2.72	31.1	84.3

2.4 Copper (Cu)

As one of the most important alloying elements, Cu is soluble in α-Al solid solution with a maximum equilibrium solubility of 5.65 wt.%. However, the typical Cu level is approximately 1 wt.% dissolved in as-cast aluminium alloys. Therefore, Cu-rich intermetallic phases are formed in the as-cast microstructure when Cu>1 wt.%, in which Al_2Cu is the main intermetallic. It is usually found in two types [87,88]: blocky θ-Al_2Cu and eutectic Al-Al_2Cu pockets in the as-cast microstructure of Al-Cu alloys, as shown in Figure 9. A high solidification rate promotes the formation of the eutectic Al_2Cu phase, while Sr modification increases the fraction of the blocky Al_2Cu phase [89].

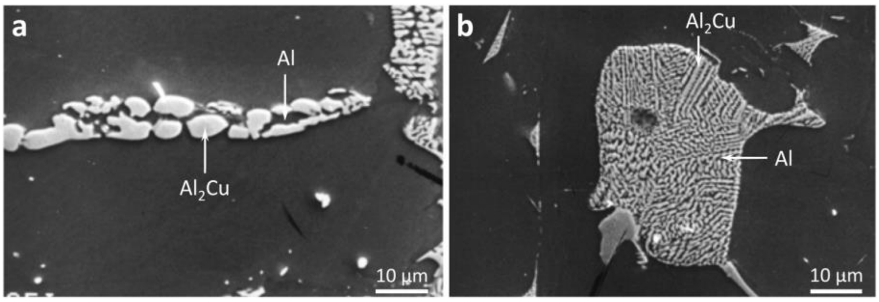

Figure 9. SEM micrographs of the as-cast Al-Cu alloy showing: (a) the blocky copper phase and (b) the eutectic copper phase [88].

Copper substantially improves the strength and hardness under as-cast and heat-treated conditions. Alloys containing 4 to 5.5 wt.% Cu respond strongly to thermal treatment and have improved casting properties. Cu atoms in the Al solid solution have a positive effect on Young's modulus. Abo-Elsoud [90] reported that the divalent Al/Cu atomic species increase the modulus of aluminium alloys when Cu is increased to ∼1 at.%, but further increases of Cu over 1 at.% decrease the Young's modulus. Dudzinski [91] found that the Young's modulus is increased by 0.56 GPa with the addition of 1 wt.% Cu in Al-Cu alloys. Eskin and Toropova [37] investigated Al-Cu binary alloys containing approximately 12-19 wt.% Cu (15-22 vol.% of the Al_2Cu phase) and found that the Young's modulus reaches 82-83 GPa in the alloys with 19 wt.% Cu.

Precipitate hardening is significant for the Young's modulus of Al-Cu alloys. Fouquet et al. [92] studied the Young's modulus affected by the θ' precipitates in the Al-4 wt.% Cu alloy, and found that a 3% increase of Young's modulus can be achieved by the formation of θ' precipitates, which is independent on the precipitate size but also significantly dependent on the volume fraction of precipitates and the coherency state at the precipitate-matrix interface. In general, the Young's modulus is increased by the increment of Cu content in the aluminium solid solution and the reinforcement effect of the θ' precipitates, decreased by the loss of coherency on the large faces of the θ' precipitates [93]. On the other hand, the increase of Cu contents in Al results in the formation of Al_2Cu intermetallic, which has a tetragonal structure and a long-range order, i.e. the elements prefer to stay on their appropriate sub-lattices. Gao [94] used empirical electron theory (EET) to verify that the covalence Al-Cu bonds in the Al_2Cu phase are stronger than that of pure Al-Al bonds, and that therefore these bonds improve the Young's modulus of the Al_2Cu phase up to 130 GPa. The presence of both long-range ordering and strong interatomic bonding of the Al_2Cu phase increase the Young's modulus of Al-Cu alloys. The Young's modulus of different volume fractions of θ-Al_2Cu (V_θ) and/or Cu contents are shown in Figure 10, together with the calculated lines from theoretical models including the rule of mixtures (1), the inverse rule of mixtures (2) and the interpolated formula (3). Obviously, increasing the Cu element in the aluminium matrix improves the modulus since the volume fraction of Al_2Cu phase increases and $E_\theta > E_{Al}$. The experimental values obtained at 1.9 and 4.7 vol.% θ-Al_2Cu exceeded the calculated values. These can be attributed to the constraints exerted on the matrix by the dispersed phase [95].

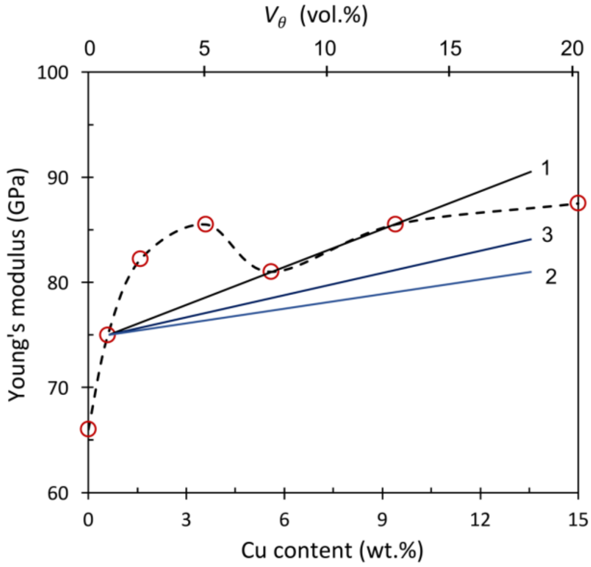

Figure 10. Variation of Young's modulus with volume fraction of the θ-Al_2Cu (V_θ) and/or Cu content. The lines 1, 2 and 3 are calculated by the rule of mixtures (ROM), the inverse rule of mixtures (IROM), and the interpolated formula, respectively [96].

In addition to Al-Cu alloys, Cu can be effective alloy elements in other cast aluminium alloys usually including Si, Mg, Zn, Zr, Ni, Mn and Ti. Cu can form a variety of ternary phases with other alloying elements. Mn in Al-Cu alloys can form $Al_{20}Cu_3Mn_2$ dispersoids in the microstructure under heat-treated conditions. Mg can be in equilibrium with the binary phase of Al_8Mg_5 and also the ternary phases of Al_2CuMg and Al_6CuMg_4 in the Al-Cu-Mg system [97]. Fe can form Al_7FeCu_2 and $Al_6(FeCu)$ phases. Cd and Ag enhance the effect of precipitate hardening. Cr and Zr, together with Mg, form dispersoids. Ni and Cu in aluminium alloys form compounds of Al_6Cu_3Ni or $Al_3(Ni,Cu)_2$. The presence of these intermetallic phases can increase the modulus of aluminium alloys. The experimentally measured Young's modulus for Al-Cu-Ni alloys are given in Table 8, together with the estimated values of the upper and lower bonds calculated from the ROM and IROM models. The phases in the alloys with highest modulus are k+θ+τ, k+τ and k+δ+τ, which are mainly determined by the composition and heat treatment process.

Table 8. Microstructural parameters and Young's modulus of Al-Cu-Ni alloys [96].

Nominal alloy addition		Type of dispersion		Volume fraction (%)		Particle size (μm)		Mean free path (μm)	Inter-particle spacing (μm)	Young's modulus (GPa)		
Ni (wt.%)	Cu (wt.%)	Phase 1	Phase 2	Phase 1	Phase 2	Phase 1	Phase 2			Ex.	ROM	IROM
1	5.7	θ	τ	10	5.7	1.9	1.0	5.2	6.7	84.5	85.4	81.2
2	10	θ	τ	3.9	17.8	3	3.8	8.1	11.5	95	92.8	84.4
3	15	θ	τ	7.1	28.9	3.5	4.1	4.5	8.3	104.9	104.3	92.1
6	1	ε	δ	12.5	3.5	1.5	1.2	4.7	6.1	97	96.4	83.5
7	2	ε	δ	4.8	11	3.6	1.3	8.6	11	95.5	93.8	83.2
8	2	ε	δ	9.5	10	1.8	1.5	4.5	6.2	94	98.8	85.2
9	2.5	ε	δ	4.3	19.5	5	1.9	7.4	10.8	94	102.0	86.7
5	10	τ	δ	28.5	1.7	5.5	2.5	6.2	10.2	94	102.0	89.7
6	8	τ	δ	0.9	16	7.5	1.5	14.7	19.2	93	93.4	93.0
7	14	τ	δ	42.5	0.25	4.8	3.7	3.8	8	98.5	112.6	97.5
8	10	τ	δ	4.5	25	11.6	22	26.1	42.9	93	105.7	88.8

The compositions and stiffness-based properties of commercially available Al-Cu alloys are shown in Table 9. Unlike the elements of Li and Be that significantly enhance the Young's modulus, Cu can slightly improve the Young's modulus of aluminium alloys. Comparing the different results, the modulus of Al-Cu binary alloys is approximately 74 GPa after adding 6 wt.% Cu. However, the simultaneous addition of Si and Cu can significantly increase the Young's modulus, as shown in Figure 11. For instance, the aluminium alloy containing 11 wt.% Si and 4 wt.% Cu shows the Young's modulus of 84 GPa [85].

Table 9. Compositions and stiffness-based properties of commercially available Al-Cu alloys [86].

Cu	Si	Mg	Mn	Fe	Ti	Zn	Cr	Ni	Zr	Pb	Al	Density (gr/cm^3)	Young's modulus
0.1		0.05	0.05			0.1					Bal.	2.70	68
0.2	0.08	0.1	1.2	0.7							Bal.	2.73	69
2.6	0.5	0.45	0.3	0.5		0.25	0.1				Bal.	2.75	71
4.0	0.5	0.6	0.7	0.7	0.15	0.25	0.1				Bal.	2.79	72
4.0	0.4	1.0	0.7	0.4		0.4				1.1		3.10	73
4.0	0.5	0.7	0.2	0.5		0.2		2.0				3.10	75
4.3	0.5	1.5	0.6	0.5	0.15	0.25	0.1		0.1		Bal.	2.78	73
4.5	0.8	0.05	0.8	1.0	0.15	0.25	0.1				Bal.	2.81	72
4.0	0.9	1.5	0.2	1.0	0.15	0.25	0.1	2.0			Bal.	2.81	74
5.0	0.3	0.05	0.2	0.5	0.2	0.3	0.1	0.4	0.2		Bal.	2.83	72
5.2	0.4			0.2						0.4		3.10	73
5.0	0.8	0.5	0.8	0.7	0.15	0.25	0.1				Bal.	2.80	73
5.0	0.7	0.5	0.8	0.5	0.15	0.25	0.1				Bal.	2.80	74
6.2	0.1		0.3	0.1					0.2			3.10	74
6.3	0.2	0.02	0.3	0.3	0.1				0.2		Bal.	2.84	74

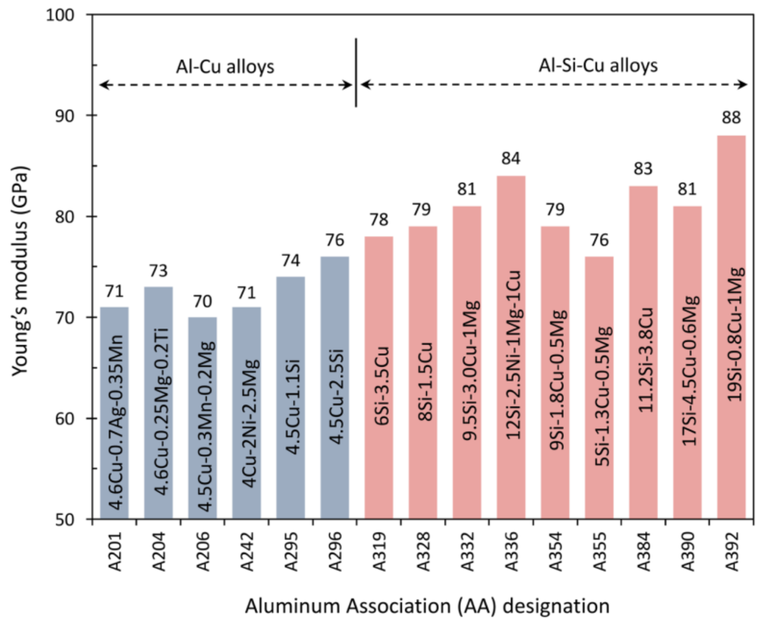

Figure 11. Young's modulus of commercial Al-Cu and Al-Si-Cu alloys [86,98].

2.5 Nickel (Ni)

According to Dudzinski [91], the Young's modulus of Al alloys increases by 1.16 GPa with the addition of each 1 wt.% Ni. Similar results (1.08 GPa/wt.% Ni) was reported by Eskin and Toropova

[37]; they showed that the Young's modulus of Al-6.5 wt.% Ni, Al-9.5 wt.% Ni and Al-12 wt.% Ni was 82, 86 and 91 GPa, respectively. The Al-12 wt.% Ni alloy containing approximately 20 vol.% Al_3Ni exhibits high elastic properties due to the intrinsic modulus of Al_3Ni, which is approximately 215 GPa [99]. The microstructure of hypoeutectic Al-Ni binary alloys consists of the ε-(Al_3Ni) phase in the aluminium matrix. The variation of the Young's modulus against the volume fraction of the ε-phase, the volume fraction of the ε-Al_2Cu (V_ε), together with the calculated lines from theoretical models are shown in Figure 12. Up to the eutectic composition, the experimental results of Young's modulus are very close to the calculated upper boundary values. The massive primary ε-phase in the hypereutectic alloys causes a noticeable decrease in the Young's modulus values, which can be attributed to the cracking from the large intermetallic compounds [96].

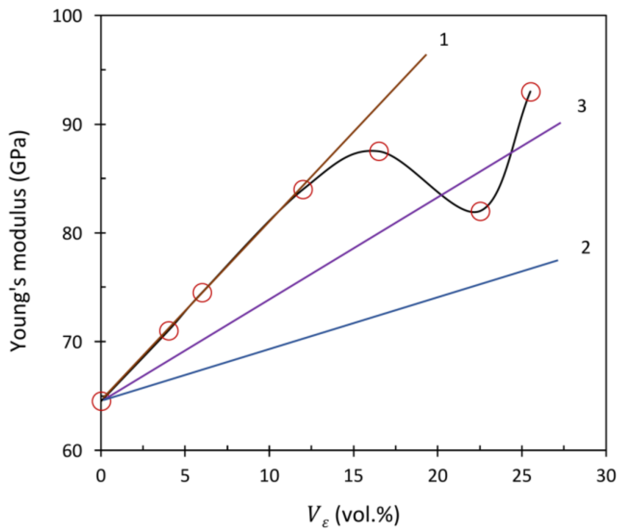

Figure 12. Variation of Young's modulus with volume fraction of the ε-Al_3Ni (V_ε) and/or Ni content. The lines 1, 2 and 3 are calculated by the rule of mixtures (ROM), inverse rule of mixtures (IROM) and the interpolated formula, respectively [96].

2.6 Chromium (Cr)

The stiffness of cast aluminium alloys is increased at a rate of 6.1 GPa/at.% by addition of Cr. This rate is the same for Cr present in Al(Cr) solid solution and in the Cr-rich intermetallic phase. Dudzinski [91] studied cast Al-Cr alloys from 0.27 to 3.2% Cr. The Cr is present in these alloys as a dispersion of $CrAl_7$ intermetallic particles. As the $CrAl_7$ intermetallic has a modulus of 130 GPa, the increase of Young's modulus can be fitted with $E_{Al-Cr} = 6.1\,\mathrm{Cr}\,(\mathrm{at.\%}) + 69$. The effect of Cr contents on the Young's modulus was also investigated by McConnell and Partridge [100,101]. They reported an increase in Young's modulus by a rate of 5.7 GPa/at.% Cr, when Cr is present as a solid solution or as intermetallic particles, i.e. $CrAl_7$ or (Cr, Fe)Al_7. The addition of Fe up to 2 wt.% to Al-Cr alloys can increase the strength and Young's modulus to ~95 GPa due to the formation of Fe-rich and Cr-rich phases.

2.7 Magnesium (Mg)

Unlike the other common alloying elements in aluminium alloys that are able to improve the Young's modulus, Mg, Na and Ca are the notable exceptions [14,30]. Under as-cast and heat-treated conditions, the Young's modulus of Al-Mg alloys is slightly decreased with increasing magnesium content. The extent of the reductions is approximately 0.5% per at.% Mg [36]. Therefore, magnesium is not a desirable addition for improving the Young's modulus. However, when the addition of Mg is greater than the maximum solubility and results in the formation of a Mg_2Si phase in the microstructure, the stiffness of the Al-Mg alloys are improved because the Young's modulus of Mg_2Si is 120 GPa [102,103]

3. Stiffness improvement in aluminium-based composites

Aluminium matrix composites (AMCs) reinforced with particles, short fibres/whiskers or continuous fibres have received considerable attention over the past decades due to the attractive properties resulting from the combination of their constituents. Al/TiB_2, Al/TiC, Al/ZrB_2, Al/SiC, Al/AlN, Al/Al_2O_3 and Al/Mg_2Si have been reported to be able to improve the Young's modulus of cast Al alloys [104,105]. The significant improvement of Young's modulus in AMCs have been successfully achieved through a variety of casting processes, including gravity casting, stirring casting, investment casting, die casting, vacuum assisted casting, semi-solid casting, and squeeze casting for manufacturing shaped components, or making billets by direct chill casting for further processing such as forging, extrusion or rolling.

The Young's modulus of pure aluminium can be enhanced from 70 to 240 GPa by the reinforcement of 60 vol.% continuous fibre [106]. Similarly, the castings of Al-9Si-20 vol.% SiC_p composites significantly improves the Young's modulus with the wear resistance equivalent or better than that of grey cast irons [107]. Discontinuously reinforced AMCs have been demonstrated to offer essentially isotropic properties with substantial improvements in stiffness and strength. However, a 50% increase in the Young's modulus of Al alloys can be achieved by substituting a discontinuous reinforcement with continuous ones in AMCs [108]. It is therefore capable of incorporating appropriate reinforcement in suitable volume fractions for casting aluminium components with improved Young's modulus and other technological properties such as high thermal conductivity, high specific strength, tailorable coefficient of thermal expansion, improved strength and low density, which is dependent upon the composition, grain size, microstructure and fabrication process.

The stiffness property of some reinforcement phases is listed in Table 10. These phases show the much-increased Young's modulus and melting point in comparison with pure aluminium. In AMCs, the reinforcement phase can be formed by in-situ reaction or by ex-situ additions. In the specific condition, the in-situ particles can act as nucleating sites for grain refinement or as strengthening phases to hinder dislocation motion [109,110]. Currently, several fabrication methods including liquid state processing, deposition process and solid state processing have been developed for the manufacture of AMCs. Figure 13 shows the detailed casting process routes for manufacturing AMCs, which include infiltration techniques [111,112], stirring techniques [113,114] and rapid solidification [115,116]. Liquid state processing is usually involved with the casting process, which is energy-efficient and cost-effective for massive production. Products of complex shape can be formed directly through the melt mixture with reinforcement. It is very attractive to produce as-cast components of AMCs with a uniform reinforcement distribution of individual particles and structural integrity. However, during solidification, the particles ahead of the interface may get pushed, engulfed or entrapped in the moving solidification front. The other difficulties in the casting process are the non-wettability of ex-situ particles by liquid metal, and the particle-Al interface interaction. Although the addition of Ni, Mg, Li, Si and Ca into Al melt can improve wettability either by changing the interfacial energy through some interfacial reaction or by modifying the oxide layer on the metal surface [117,118,119], the difficulty to obtain uniform dispersion of reinforcement particles is still an issue that hinders the adoption of AMCs in industry [120,121].

In order to effectively improve the Young's modulus of AMCs, the generation of high modulus phases, the reinforcement phases with covalent and ionic interatomic bonds in aluminium alloys are preferred approaches according the nature of stiffness [122,123]. Therefore, the in-situ method is better than the ex-situ method because the wettability between the in-situ formed phases and the aluminium matrix is significantly higher and is capable of forming clean and strong interfacial bonding in between [124,125]. However, the in-situ method is suitable for particulate reinforced AMCs because the in-situ techniques are not capable of making continuous fibre reinforced AMCs.

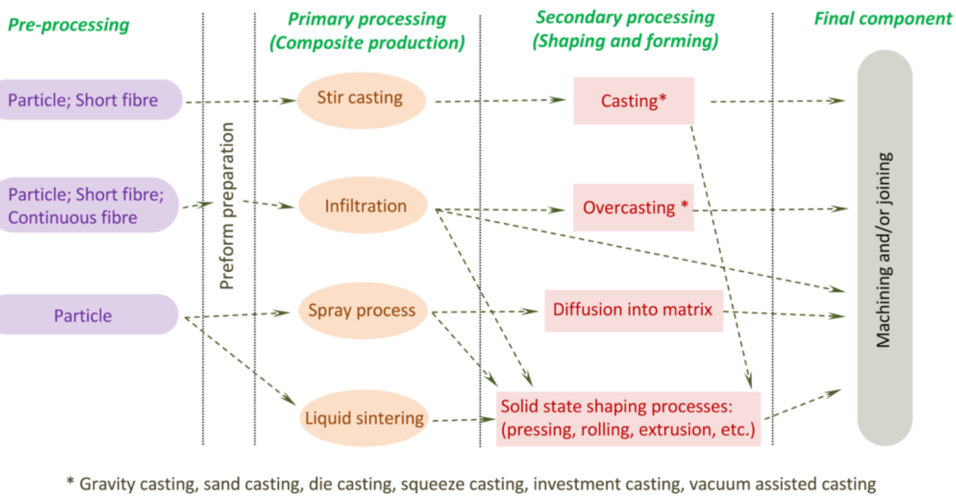

Figure 13. Schematic diagram of processing methods of AMCs.

Table 10. Properties of typical reinforcements [126,127,128].

Reinforcement	Melting point (ºC)	Young's modulus (GPa)	UTS (MPa)	Density (g/cm^3)	Thermal conductivity (W/m·K)	Coff. of thermal expansion (10^{-6}/K)
ZrB_2	3,246	350		6.09	140	7.4
AlN	2,200	330	2,100	3.26	150	3.3
Al_2O_3	2,043	380	2,070	3.15	30	7.0
TiC	3,067	400	1,540	4.90	110	9.0
TiB_2	3,225	560	3,300	4.52	24	8.0
Mg_2Si	1,102	120		4.50	4.4	7.5
ZrO_2	2,715	350	2,070	4.84	3.3	7.0
B_4C	2,763	425	2,690	2.35	39	3.5
SiC	2,730	450	2,280	3.21	120	3.4
VC	2,810	430		5.77		4.1
WC	2,870	640	500	15.52	60	5.1
Si_3N_4	1,900	207	530	3.18	28	1.5

The Young's modulus of composite materials can be estimated by theoretical modelling, which depends on the morphological arrangement of materials components. The most frequently used mathematical models include: (1) the rule of mixtures (ROM) and the inverse rule of mixtures (IROM) [129], (2) the Halpin-Tsai model [130], (3) the Hashin-Shtrikman model [131] and (4) the Tuchinskii model [132]. The ROM (upper bound) and IROM (lower bound) can be obtained according to the equal strain assumption and the equal stress assumption, respectively [133]. The elastic properties of all of the composites are usually located between the ROM upper and IROM lower bounds [134]. The Halpin-Tsai model has a more complicated mathematical structure than that of the ROM or IROM. In this model, the modulus of elasticity and the volume fraction of the components and the aspect ratio (ratio of the geometric dimensions) of the reinforcement are taken into account. It has been widely reported that Halpin-Tsai model is more accurate for particulate metal matrix composites. In the Hashin and Shtrikman (H-S) theorem [131], the upper bound rigorously corresponds to the composites containing the 'soft' inclusion matrix phase encapsulated by a 'stiffer' reinforcement phase, while the lower bound corresponds to the composites with a 'stiffer' inclusion reinforcement phase encapsulated by a 'softer' matrix phase. The H-S bounds are tighter than the ROM bounds and have been regarded as the best possible bounds on properties for isotropic two-phase composites. The Tuchinskii model [132] considers a two-phase interpenetrating skeletal structure. The calculated value of modulus can be a good estimation of experimental guidance. However, this review will not focus the modelling approaches and principles. Some existing results from modelling are used to review the experimental data.

3.1 Al/TiB_2 composites

TiB_2 is one of the most popular reinforcements for high modulus AMCs because of its Young's modulus of 560 GPa and its easy synthesis using an in-situ process. The in-situ formed TiB_2 offers a better interface with the aluminium matrix than the ex-situ added particles [135,136]. The in-situ Al/TiB_2 composites can be synthesised using K_2TiF_6 and KBF_4 salt reactions in molten Al [137]; through a self-propagating high-temperature synthesis (SHS) reaction via Al-Ti-B powder compact/preform added to molten Al [138,139,140]; through the reaction of TiO_2-H_3BO_3-Na_3AlF_6 with Al [141]; or via chemical reactions among Al, TiO_2 and B_2O_3 particles [142]. It is generally believed that the presence of a Al_3Ti phase in Al/TiB_2 composites is beneficial for grain refinement but is detrimental to the mechanical properties [143]. The Al_3Ti can be eliminated during synthesis by the proper control of temperature, time and ratios of the raw materials [144,145]. The presence of Si in cast Al alloys can improve the dispersion of TiB_2 particles [146], although the TiB_2 particles are still partially segregated in the eutectic regions because of the pushing mechanism during solidification [147,148,149]. The typical microstructure of Al/TiB_2 composites is shown in Figure 14. The Al-9Si-1Mg-0.7Cu/TiB_2 composite can be produced with clean, smooth and well-bonded interfaces between the aluminium matrix and TiB_2 particles between 25 and 3,000 nm [150].

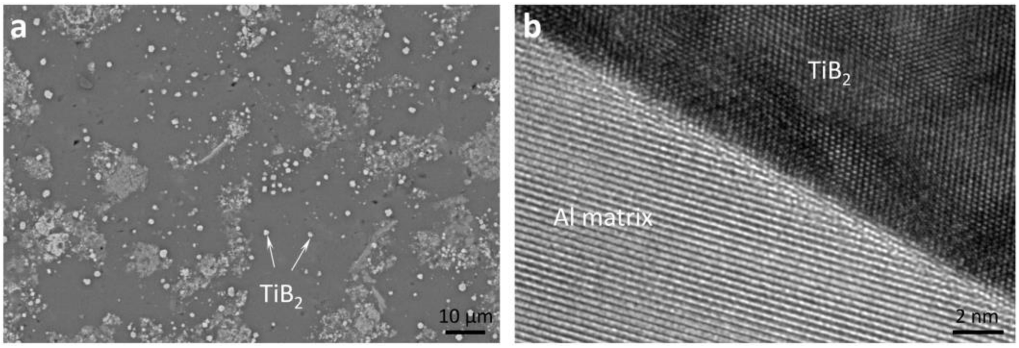

Figure 14. (a) A SEM micrograph of the Al-9Si-1Mg-0.7Cu/TiB_2 composite with 14 wt.% TiB_2 particles and (b) a TEM micrograph showing the clean and well-bonded interface between the α-Al and TiB_2 particles [150].

The TiB_2 reinforced AMCs can remarkably improve the mechanical properties, in particular the stiffness. The typical Young's modulus and other mechanical properties of particulate reinforced Al/TiB_2 composites are summarised in Table 11. The increase of the Young's modulus of Al/TiB_2 composites can be up to 40% higher than that of pure aluminium [151,152]. The strength at elevated temperatures and the wear and fatigue resistance can also have a significant increase [151]. Kumar et al. [153] reported an increase of 108% in hardness, 123% in yield strength, 43% in UTS and 33% in Young's modulus of the Al-7Si cast alloy with 10 wt.% of TiB_2, which provides a Young's modulus greater than 90 GPa. Han et al. [154] studied the tensile properties of the Al-12Si alloy with 4 wt.% TiB_2 particles and found that the improvement of the Young's modulus can be observed in the temperature range of 25-350 °C. Amirkhanlou et al. [150] reported that Al-9Si-1Mg-0.7Cu/9 vol.% TiB_2 can provide a Young's modulus greater than 94 GPa and the yield strength up to 235 MPa by the formation of α-Al (Cu, Mg), Si and TiB_2 phases in the microstructure. Lu et al. [155] investigated the Al/TiB_2 composite and found that the Young's modulus reaches 107 GPa by adding 15% TiB_2 into the Al matrix.

Table 11. Mechanical properties of Al/TiB_2 cast composites synthesised by K_2TiF_6 and KBF_4 salt reaction [153,154,156,157].

Materials	Temperature (°C)	Young's modulus (GPa)	0.2% Proof stress (MPa)	UTS (MPa)	Elongation (%)
Al-7Si/5 vol.% TiB_2	25	83.0	126	175	7.00
Al-7Si/10 vol.% TiB_2	25	92.0	152	209	4.60
Al-12Si/4 wt.% TiB_2	25	85.0	240	298	1.50
Al-12Si/4 wt.% TiB_2	200	80.0	189	233	3.00
Al-12Si/4 wt.% TiB_2	350	66.0	84	96	5.80
A356/2.1 vol% TiB_2	25	72.9	209	235	7.81
A356/4.7 vol% TiB_2	25	76.3	212	252	7.36
A356/8.4 vol% TiB_2	25	82.2	217	258	2.73
A356/2.1 vol% TiB_2	25	78.1	305	375	4.88
A356/4.7 vol% TiB_2	25	80.2	317	377	1.90
A356/8.4 vol% TiB_2	25	84.1	347	391	1.32
Al/5 vol.% TiB_2	25	69.0	188	284	3.50
Al/10 vol.% TiB_2	25	84.0	249	326	1.92
Al/5 vol.% TiB_2	25	82.0	96	124	9.20
Al/10 vol.% TiB_2	25	87.0	128	164	6.30
Al/15 vol.% TiB_2	25	91.0	124	153	5.50
Al-Cu/10 vol.% TiB_2	25	77.0	153	230	5.50
Al-Cu/10 vol.% TiB_2	25	83.0	311	361	1.30
Al/15 vol.% TiB_2	25	107.0	274	389	1.99
Al/15 vol.% TiB_2	25	91.0	171	223	4.60
Al-Cu/15 vol.% TiB_2	25	93.0	248	333	2.30

3.2 Al/TiC composites

Titanium carbide (TiC) is a hard refractory ceramic material with FCC crystal structures. The Young's modulus is approximately 400 GPa and the shear modulus is 188 GPa for the TiC [158,159], which is a good candidate as reinforcement for improving stiffness of aluminium alloys [160]. Al/TiC in-situ composites can be synthesised by several techniques, including: (a) the reaction of K_2TiF_6 salt and graphite, (b) the direct reaction of Ti and C powders, (c) the addition of Al-Ti-C powder into the Al melt, and (d) the reaction of CH_4 gas with the Al-Ti melt. The reactions can be at a level of 1,000ºC for 30 minutes for Al-4.5 Cu alloys [161,162]. The in-situ formed TiC particles can be smaller than 1 µm in size or in a range of several micrometers [162,163]. The formation of other phases, such as Al_4C_3 and Al_3Ti phases, is considered to be unfavourable in Al/TiC composites [164,165].

On top of the enhancement of mechanical properties, the addition of TiC particles into aluminium melt has a dramatic improvement on the Young's modulus, as shown in Figure 15. Samer et al. [166] obtained the Young's modulus of 106 GPa, the yield strength of 450 MPa and the elongation of 6% in the composites containing 22 vol.% TiC in pure Al. Mohapatra et al. [167] confirmed that the Young's modulus is increased from 70 GPa of pure aluminium to 88.78 GPa after adding 20 vol.% TiC. The mechanical properties of Al-4.5%Cu alloy reinforced with different amounts of TiC are summarised in Table 12, in which the addition of 10 wt.% TiC increases the Young's modulus to 99 GPa [168]. In addition, the Young's modulus of the Al/TiC composite is close to the upper limit calculated from the Hashin-Shtrikman model [169,170], suggesting that the in-situ synthesis of TiC particles leads to strong interfacial bonding and the attendant load transfer. Despite the high stiffness of Al/TiC in-situ composites, the porosity level and other oxide impurities in the melt are the main concerns because of the high synthesis temperature of 1,000-1,200 ºC. This also results in limitations for the industrial applications of in-situ Al/TiC composites.

Table 12. Mechanical properties of Al matrix and Al-4.5Cu/TiC in-situ composites [171].

Materials	Vickers hardness (HV5)	Young's modulus (GPa)	Yield strength (MPa)	UTS (MPa)
Al-4.5%Cu	55.19	72.8	81.5	118
Al-4.5Cu/5wt.% TiC	61.12	83.4	95.7	134
Al-4.5Cu/7wt.% TiC	69.43	91.8	103.4	156
Al-4.5Cu/10wt.% TiC	75.76	98.7	117.3	179

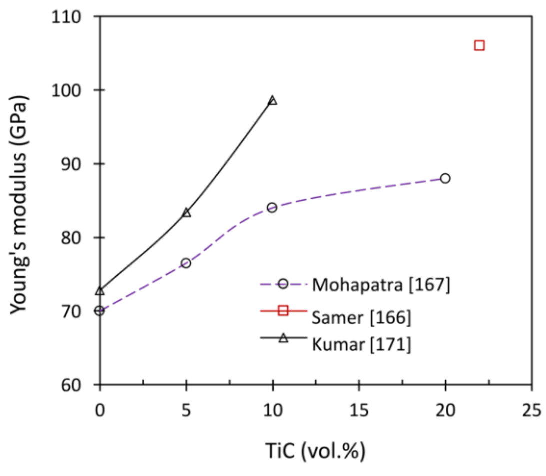

Figure 15. Effect of TiC on the Young's modulus of Al/TiC composites.

3.3 Al/SiC composites

SiC reinforcements are usually added into Al melt through ex-situ additions incorporating with stirring or mixing. Casting routes can be gravity casting and squeeze casting. Alternatively, the alloy is infiltrated into a porous preform formed by SiC reinforcements. The wettability between the SiC reinforcements and the aluminium alloy is a crucial concern in association with the optimum fluidity of the alloy. One of the main problems during the processing and casting of Al/SiC composites is that liquid aluminium attacks SiC reinforcements through chemical reaction, forming Al_4C_3 and Si [172]. Particle clustering has greater effects on the flow behaviour and mechanical properties of Al/SiC AMCs because the particle clustering microstructure experiences a higher percentage of particle fracture than that with particle random distribution [173]. The stirring casting is an effective way to promote the distribution of ex-situ particles [174,175].

Table 13 summarises the Young's modulus and mechanical properties of ex-situ Al/SiC AMCs. The Young's modulus of the AMCs with cast aluminium alloys can be enhanced to 114 GPa when the reinforcement is at a level of 20 vol.%. The castibility is a significant concern when the SiC addition is beyond this level. For wrought aluminium alloys, the addition of SiC reinforcement can be at a level of 25 vol.% for casting and the subsequent plastic deformation processing. The Young's modulus can be 140 GPa, which is double the Young's modulus of pure aluminum.

Table 13. Young's modulus and mechanical properties of ex-situ Al/SiC AMCs [108,176].

Materials	Reinforcement	Casting method	Young's modulus (GPa)	Yield strength (MPa)	UTS (MPa)	Elongation (%)
Al-10Si-3Cu-1Mg-1.25Ni	10 vol.% SiC	Gravity	88	359	372	0.3
Al-10Si-3Cu-1Mg-1.25Ni	20 vol.% SiC	Gravity	101	372	372	0.1
Al-9Si-0.5Mg	10 vol.% SiC	Gravity	86	303	338	1.2
Al-9Si-0.5Mg	20 vol.% SiC	Gravity	99	338	359	0.4
Al-10Si-1Fe-0.6 Mn	10 vol.% SiC	Pressure die cast	91	221	310	0.9
Al-10Si-1Fe-0.6 Mn	20 vol.% SiC	Pressure die cast	108	248	303	0.5
Al-10Si-3.25Cu-1Fe-0.6 Mn	10 vol.% SiC	Pressure die cast	94	241	345	1.2
Al-3.25Cu-1Fe-0.6 Mn	20 vol.% SiC	Pressure die cast	114	303	352	0.4
A356	10 vol.% SiC	Casting	81	283	303	0.6
A356	15 vol.% SiC	Casting	90	324	331	0.3
A356	20 vol.% SiC	Casting	97	331	352	0.4
Al-12Si-Ni-Cu	20 vol.% SiC	Squeeze casting	111	293	384	
Al-7Si-Mg-Fe	15 vol.% SiC	Gravity	98	183	280	1.0
Al-3Mg	20 vol.% SiC	Gravity	105	377	408	1.4
Al-4.4Cu-Si-Mg	15 vol.% SiC	Gravity	107	342	350	1.6
Al-7Si-0.3Mg	10 vol.% SiC	Casting	82	287	308	0.6
Al-7Si-0.3Mg	15 vol.% SiC	Casting	91	329	336	0.3
Al-7Si-0.3Mg	20 vol.% SiC	Casting	98	336	357	0.4
A380	10 vol.% SiC	Casting	95	245	332	1.0
A380	20 vol.% SiC	Casting	114	308	356	0.4
AA6061	20 vol.% SiC	Casting-forming	119	448	551	1.4
AA6061	20 vol.% SiC	Casting-extrusion	108	414	545	2.0
AA6061	20 vol.% SiC	Casting-hot rolling	104	402	550	4.5
AA2014	15 vol.% SiC	Casting-forming	100	466	493	2.0

AA2024	20 vol.% SiC	Casting-forming	110	465	620	2.0
AA2024	25 vol.% SiC	Casting-forming	140	470	800	2.0
AA2024	15 vol.% SiC	Casting-hot rolling	96		530	2.4
AA2024	15 vol.% SiC	Casting-hot rolling	110		330	1.2
AA2618	12 vol.% SiC	Casting-forming	98	460	532	3.0
AA2124	17.8 vol.% SiC	Casting-forming	100	400	610	6.0
AA2124	20 vol.% SiC	Casting-forming	105	405	560	7.0
AA2124	25 vol.% SiC	Casting-forming	116	490	630	3.0
AA7075	15 vol.% SiC	Casting-forming	95	556	601	3.0
AA7075	15 vol.% SiC	Casting-forming	90	598	643	2.0
AA7075	20 vol.% SiC	Casting-forming	105	665	735	2.0
AA8090	13 vol.% SiC	Casting-forming	101	455	520	4.0
AA8090	13 vol.% SiC	Casting-forming	101	499	547	3.0
AA8090	17 vol.% SiC	Casting-forming	105	310	460	5.5
AA8090	17 vol.% SiC	Casting-forming	105	450	540	3.5

3.4 Al/AlN composites

Aluminium nitride (AlN) has a Young's modulus of 310 GPa and therefore it can fairly increase the modulus of aluminium castings [177,178]. However, because of the low thermal expansion and good thermal conductivity, Al/AlN is attractive in some specific applications. In-situ Al/AlN composites are usually made by a direct reaction between N_2 and/or NH_3 gas with the molten aluminium alloys [179,180]. The nitridation of Al is a thermodynamically exothermic process and is energetically favourable over an extensive temperature range. The formed AlN particles are smaller than 10 µm and show a hexagonal morphology [181,182]. The AlN particles can be less than 2 µm in the Al/AlN composites synthesised by adding NH_3 into the melt in the temperature range from 1,100 to 1,270ºC [183]. In comparison with the purified N_2 bubbling gas, NH_3 can enhance the formation of the AlN phase in aluminium melt [183]. Chedru [184] studied ex-situ Al/AlN AMCs with squeeze casting and found that Al/AlN composites can significantly improve the mechanical properties, as shown in Table 14. Balog [185] studied Al/AlN AMCs with cold isostatic pressing (CIP) and extrusion, and the results are shown in Figure 16. The Young's modulus is significantly increased when increasing the content of AlN in the AMCs. However, the studies for castable materials are still very limited.

Table 14. Young's modulus and shear modulus of reinforced and non-reinforced materials [184].

	Young's modulus (GPa)	Shear modulus (GPa)
Al-4Cu-1Mg	72.9	27.1
Al-4Cu-1Mg/45%AlN	146.3	56.5
Al-1Mg-0.5Si	72.5	27.1
Al-1Mg-0.5Si/42%AlN	141.3	54.6
Al-3Mg	71.3	26.6
Al-3Mg/48%AlN	149.5	58.2

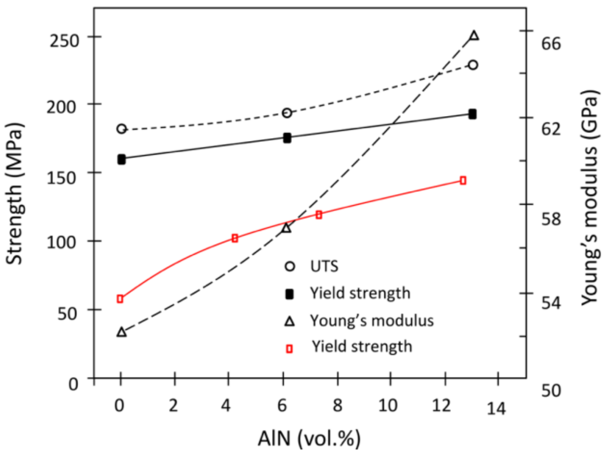

Figure 16. Ultimate tensile strength (UTS), yield strength and Young's modulus of Al-AlN nanocomposites prepared by CIP with subsequent extrusion [185].

3.5 Al/ZrB$_2$-Al$_3$Zr composites

Al/ZrB$_2$-Al$_3$Zr composites use the hybrid reinforcement phases of ZrB$_2$ and Al$_3$Zr. The Young's modulus is 350 GPa for ZrB$_2$ and 205 GPa for Al$_3$Zr. Al/ZrB$_2$-Al$_3$Zr in-situ composites are usually synthesised by the addition of K$_2$ZrF$_6$ and KBF$_4$ salts to Al melt [186]. Zhang et al. [187] synthesised in-situ ZrB$_2$ and Al$_3$Zr particles in A356 alloy with K$_2$ZrF$_6$ and KBF$_4$ salts. The ZrB$_2$ and Al$_3$Zr particles are from 0.3 to 0.5 μm, as shown in Figure 17. Zhao et al. [188] reported that the morphologies of Al$_3$Zr are sensitive to the temperature of the Al melt. When the temperatures change from 850 to 1,000ºC, the morphologies of the Al$_3$Zr particles can be spherical-shape, tetragon-shape, rod-shape and fibre-shape, but the ZrB$_2$ particles show no obvious diversity in morphology. The particulate reinforced Al/ ZrB$_2$-TiB$_2$ composites can also be formed by the addition of KBF$_4$, K$_2$ZrF$_6$ and K$_2$TiF$_6$ salts into Al melt [189,190], by which the formed TiB$_2$ and ZrB$_2$ particles are hexagonal with the average size less than 2 μm [191].

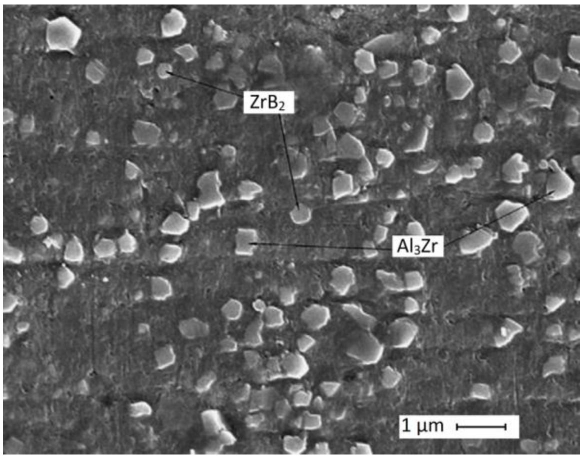

Figure 17. SEM image of the Al/ZrB$_2$-Al$_3$Zr hybrid composite.

The Al/ZrB_2-Al_3Zr composites show valuable improvement in stiffness, strength and wear properties with the increase in ZrB_2 contents [192,193]. As shown in Figure 18, Selvam and Dinaharan [194] verified the stiffness improvement of 7075/ZrB_2 composite, which is further attributed to ZrB_2 that has a covalent interatomic bond and high intrinsic modulus. However, Gautam et al. [195,196] found that the improvement of the Young's modulus in Al/ZrB_2-Al_3Zr hybrid composite is insignificant when the volume fraction of ZrB_2 particles increases.

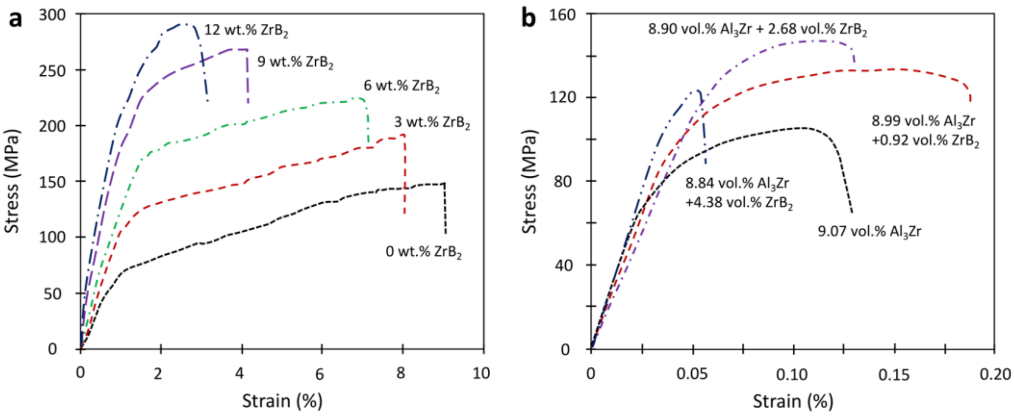

Figure 18. Stress-strain graphs showing: (a) the effect of ZrB_2 content in AA7075/ZrB_2 in-situ composites and (b) the effect of ZrB_2 and Al_3Zr content in AA5052/ZrB_2-Al_3Zr in-situ composites [195, 196].

3.6 Other particulate reinforced AMCs

The other typical reinforcements listed in Table 10 are capable of being synthesised by in-situ reactions. However, the compounds with high modulus are more attractive. In addition to that described in the previous section, Al_2O_3, WC, B_4C and VC are also good candidates for improving the Young's modulus of aluminium composites. For example, the in-situ Al/Al_2O_3 composites can be synthesised by: (a) the direct melt oxidation of aluminium alloys at high temperature [197], (b) directly passing oxygen into the aluminium melt to form Al_2O_3 [198], and (c) the displacement reactions between metal oxides and aluminium to produce Al_2O_3 particulate reinforcement. However, the experimental evidence for the improvement of Young's modulus in those in-situ AMCs is not sufficient.

The manufacture and the properties of ex-situ AMCs have been comprehensively reviewed by Rohatgi et al. [199]. Al/SiC and Al/TiB_2 have also been discussed in the present paper. The other ex-situ AMCs processed by casting methods are shown in Table 15. It is possible to combine up to 20 vol.% of $A1_2O_3$ into different aluminium alloys for improving the Young's modulus. The dominant factors in controlling the Young's modulus of ex-situ AMCs are the type, shape, volume fraction and distribution of reinforcement phases. The porosity and other microstructural characteristics are also critical for property improvement [200,201]. The presence of matrix-particle decohesion, particle cracking and void growth can decrease the load transfer capability of the interface and, consequently, decrease the Young's modulus of the AMCs. The subsequent mechanical processes are an effective approach to enhance the quality of the interface between matrix and reinforcement in ex-situ cast composites as well as the distribution of high modulus particles, as shown in Table 15. Secondary plastic deformation isn't capable of altering the Young's modulus of AMCs [202]; however, these processes can improve the toughness of the composites.

The main concern on the Young's modulus of ex-situ AMCs is their tendency to have relatively low ductility and fracture toughness, as shown in Table 15. The damage mechanism of ex-situ AMCs is mainly the reinforcement fracture and decohesion at the matrix/reinforcement interface. To achieve acceptable ductility and toughness, the composition, heat treatment process, size and shape distribution of the reinforcement should be precisely controlled. Also, secondary mechanical deformation will result in an improvement of ductility. In the presence of strong interfacial bonding, effective load transfer from the matrix to the reinforcement is enhanced, leading to good ductility and damage resistance.

Table 15. Young's modulus and mechanical properties of Al-based particulate ex-situ composites [20,107,176].

Materials	Reinforcement	Casting method	Young's modulus (GPa)	YS (MPa)	UTS (MPa)	Elongation (%)
Al-12Si-Ni-Cu	20 vol.% Al_2O_3	Squeeze casting	95	210	297	
Al-4.2Cu-1.4Mg-0.6Ag	25 vol.% Al_2O_3	Stir casting-forming	97	450	460	0.5
Al-4Cu-1Mg-0.5Ag	15 vol.% Al_2O_3	Stir casting-forming	90	414	510	1.3
A201	20 vol.% TiC	Stir casting-forming	105	420		2.0
AA6061	10 vol.% Al_2O_3	Stir casting-forming	81	297	338	7.6
AA6061	15 vol.% Al_2O_3	Stir casting-forming	88	386	359	5.4
AA6061	20 vol.% Al_2O_3	Stir casting-forming	99	359	379	2.1
AA6061	15 vol.% Al_2O_3	Casting-forming	91	342	364	3.2
AA6061	15 vol.% Al_2O_3	Casting-forming	98	405	460	7.0
AA6061	20 vol.% Al_2O_3	Casting-forming	105	420	500	5.0
AA6061	25 vol.% Al_2O_3	Casting-forming	115	430	515	4.0
AA2014	10 vol.% Al_2O_3	Stir casting-forming	84	483	517	3.3
AA2014	15 vol.% Al_2O_3	Stir casting-forming	92	476	503	2.3
AA2014	20 vol.% Al_2O_3	Stir casting-forming	101	483	503	0.9

3.7 AMCs with continuous reinforcement

Al alloys reinforced with continuous ceramic reinforcement, such as SiC and Al_2O_3, can be considered as alternative materials to achieve outstanding specific strength and modulus. The Al/SiC_p and Al/Al_2O_3 composites can be produced by the molten aluminium infiltration techniques, such as pressure assisted, vacuum driven and pressureless or capillarity driven processes. Aghajanian et al.

[203,204] reported the pressureless infiltration technique, by which the aluminium alloys infiltrated the reinforcement preforms spontaneously in a nitrogen atmosphere. This method is believed to be a cost-effective, nearly-net shape technique with the combined processing of materials and shaping of the components simultaneously.

The basic problem encountered in the fabrication of these composites is the rejection of the ceramic phase by the liquid metal due to their lack of wettability [205]. To improve the wetting of ceramics by liquid metals, a possible approach is to apply a metal coating on the ceramic particles, which essentially increases the overall surface energy of the solid, thereby promoting wetting by the liquid metal. Although, the continuous ceramic reinforcement/fibres can provide 210 GPa Young's modulus [206], they usually suffer from very low ductility – less than 0.2 – restricting their applications. Moreover, it is difficult to make shaped castings.

4 The Young's modulus of hybrid materials

Hybrid materials can be considered as a special type of composites, in which continuous metallic wires/bars are used as skeletons or frames for overcasting with conventional casting methods [207,208]. The network structures, or skeletons or continuous fibres, have been extensively used in polymer/ceramic matrix composites [209,210], but the hybrid materials are particularly used in this review for the metal-metal mixture made by overcasting, in which the metallic skeletons or frames made by high modulus reinforcement are covered partially or completely by aluminium alloys. The skeleton preforms not only provide a controlled and stable reinforcement, but also offer new architectures and increase the Young's modulus and provide more effective load transfer [211].

Compared with the reinforcements such as particles [212], whiskers [213], short fibres and continuous fibres [214] used in AMCs, the metallic network structures or skeletons are likely desirable to perform more efficiently, especially in reinforcing the local area of a cast component with relatively low cost and more flexible in manufacturing through overcasting. AMCs usually present low fracture toughness due to the brittle nature of reinforcement, which restricts their applications. The network structure fabricated by metallic wires can be 1D, 2D or 3D interconnected structures with appropriate surface treatment, which enhance the interface bonding by overcasting and improve the modulus without scarifying ductility and toughness. The network structure and the interface are two critical aspects for the manufacturing of sound hybrid materials. According to the nature of metals, nickel and steel/iron are two popular options for making network structure in the existing literature. Limited studies for other potential metals have been performed.

4.1 Al/Nickel hybrid materials

The interconnected network made by continuous wires of Inconel 601 (12 μm diameter) has been used to reinforce aluminium alloys through sintering the wires before infiltrating aluminium melt by squeeze casting [215,216]. Figure 19a shows the stress-strain curves for pure Al and Al/Ni hybrid materials [217]. The remarkable improvement of ductility is attributed to the absence of defects in the microstructure of the Al/Ni hybrid materials. Figure 19b shows the variation of the Young's modulus of Al/Ni hybrid materials as a function of the volume fraction of the reinforced wires, in which the upper and lower curves correspond to the ROM and IROM models computed using E_{Al}=70 GPa and E_{In601}=206 GPa. The Young's modulus increases in the hybrid materials with increasing the Ni volume fraction. Most of the results are close to the average between the two bounds defined by the ROM and IROM models. The Young's modulus can reach a level of 95 GPa, while the elongation is still more than 7% in the Al/30 vol.% Ni wire reinforced hybrid materials [216]. The deformation has no significant effect on the Young's modulus of the Al/Ni hybrid materials, as shown in Figure 20. The Young's modulus under as-cast condition is very similar to that under as-deformed condition [217], which is due to the fact that heat-treatment and metal forming don't change the volume fraction of high modulus phases in the aluminium alloys and thereby negligible change has been reported after these processes [218].

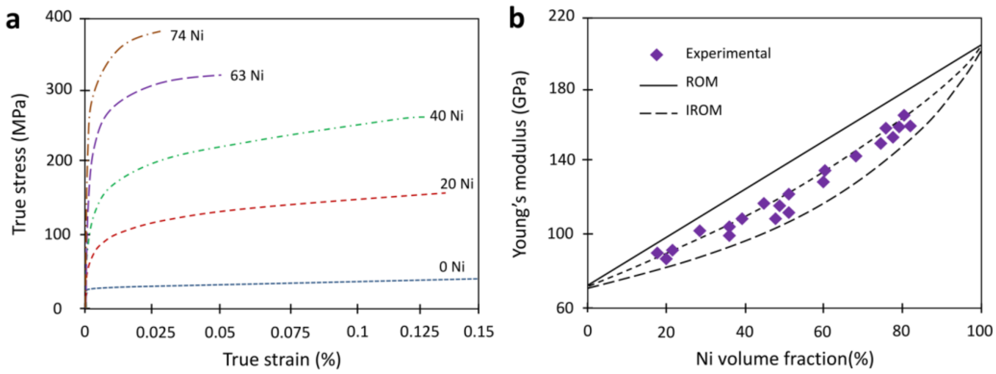

Figure 19. (a) Tensile curves and (b) Young's modulus of pure Al and Al/Ni hybrid materials [217].

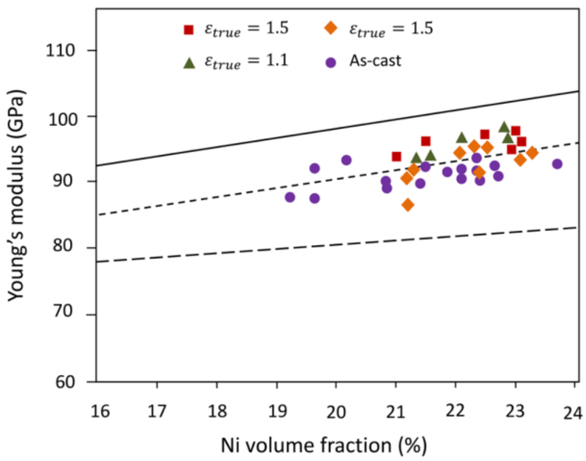

Figure 20. Young's modulus of as-cast and deformed Al/Ni hybrid materials [219].

The interface between Al matrix and wire reinforcement plays a critical role in stiffness enhancement in the hybrid materials. Salmon et al. [219] investigated the influence of the oxidation of Ni wire on the mechanical properties of Al/Ni hybrid materials and found that an optimum stress and ductility can be obtained with an appropriate oxidation of the Ni alloy during sintering. The mechanical properties can be justified as a result of compromise between the sufficient oxide roughness to the desired wire/matrix adhesion and the limited oxidation to prevent an excessive degradation of the wires. The tensile properties of Al/Ni hybrid materials are sensitively affected by the nature of the layer of oxide barrier which protects the wires from the reaction with the matrix during overcasting [220]. The ductility of Al/Ni hybrid materials can be improved by tuning the annealing conditions during the sintering process and introducing a barrier layer into the Al/Ni interface. It has been found that the partial conversion of the barrier layer into a mixture of Al_2O_3+Cr_2O_3 oxides forms the precipitation of a layer of $NiAl_3$ grains on top of the oxide layer, as shown in Figure 21 [215]. When the reduction process of Ni and Fe oxides by Al is completed, Al can diffuse across the oxide layer to form aluminide nodules by reacting with the constituents of the Ni wire. The formation of these nodules can increase the flow strength and the ductility in Al/Ni hybrid materials [215,220].

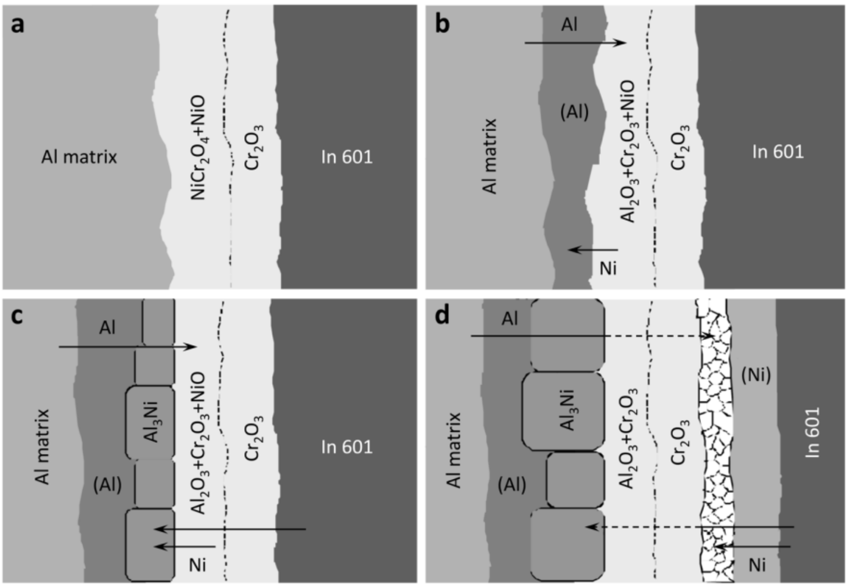

Figure 21. Mechanism of nucleation and growth of the intermetallic nodules in the Al/Ni hybrid materials [220].

The matrix materials also affect the Young's modulus of the hybrid materials. Boland et al. [221] investigated the stiffness of cast Al-13 wt.% Si alloy reinforced by Inconel 601 wires. As shown in Figure 22, the Young's modulus can be significantly increased with the increment of Ni contents in the Al-13 wt.% Si alloy. Comparing the results shown in Figure 19 to Figure 22, the reinforcement is more effective in the alloys than that in the pure aluminium.

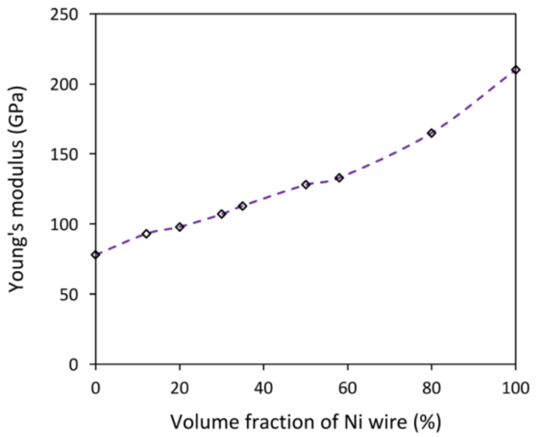

Figure 22. Young’s modulus of Al-13 wt.% Si alloy reinforced with Ni wires [215].

Two parameters are important in the processing of hybrid materials. One is the initiation of a reaction between the wires and the matrix, which is normally controlled by the cooling rate during casting, and the second is the stability of the oxide passivation barrier at the surface of the wires. The stability of the oxide barrier can be increased either by a pre-oxidising treatment for the reinforcement wires or by specified alloying elements to decrease the melting temperature of the matrix. The Cr-rich passivation layer on the surface of IN601 can increase the refractoriness in oxidising environments. This will reduce the reactivity of the wires toward Al during overcasting. On the other hand, when the matrix is Al-Si alloys, the Si platelets tend to nucleate preferentially at the wire/matrix interface. This phenomenon has been reported to occur commonly in the composites with SiC, Al_2O_3 or TiB_2 reinforcements with the particle pushing mechanism [220]. Therefore, the presence of Si in Al induces a strong reduction of the reactivity between the wires and the matrix, which can result in the further improvement in the Young’s modulus of the hybrid materials. As illustrated in Figure 23, no reaction compound in the matrix could be detected in the hybrid materials processed using optimised pre-oxidised preforms [15]. It is necessary to note that the interface requirement is different between the AMCs and the hybrid materials. In AMCs, the interface is preferred to be clean without any reaction. However, a limited reaction layer is preferred in the hybrid materials for the better mechanical properties.

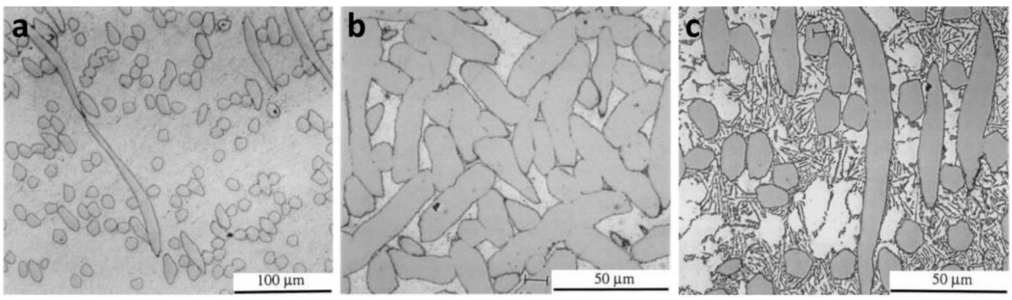

Figure 23. Optical micrograph of (a) Al/20 vol.% Ni, (b) Al/80 vol.% Ni and (c) Al-13Si/20 vol.% Ni hybrid materials [215].

4.2 Al/stainless steel hybrid materials

Fabrication of aluminium-based hybrid materials reinforced by 3D entangled stainless steel wires has been successful using mono-filament annealed 304 stainless steel wires with 100 µm in diameter in a preform structure [222,223]. The continuous wire was firstly coiled around a ø1.5 mm rod to form spring-like segments, which were subsequently stretched and entangled to form a pre-compacted sample for squeeze casting. The nominal compressive stress-strain curves are shown in Figure 24. The yield strength and the Young's modulus of the hybrid material increase as the volume fraction of the steel wires increases. The yield strength can reach 318 MPa for the hybrid material reinforced with the 35.4 vol.% of entangled stainless steel preform. The Young's modulus of Al/26 vol.% stainless steel hybrid material is 124 GPa, which shows a significant improvement in comparison with that of the A356 alloy.

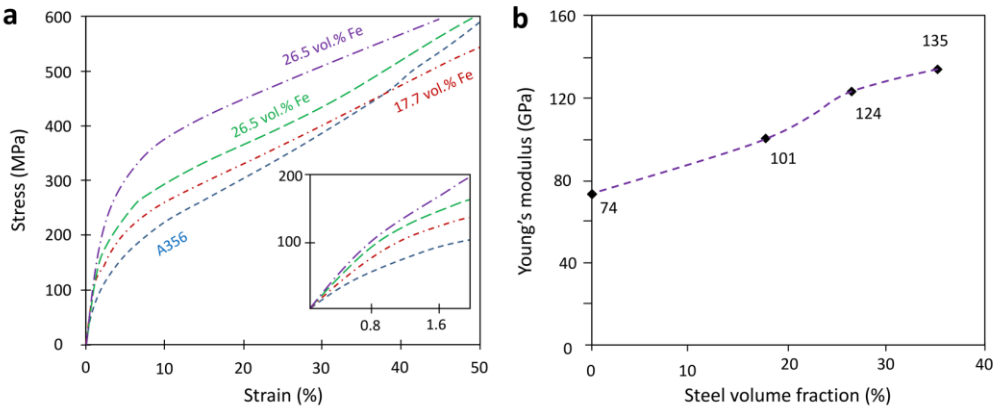

Figure 24. (a) Stress-strain curves for the hybrid materials with different volume fraction of steel wires and (b) the corresponding Young's modulus [222].

The microstructures of A356 matrix alloy reinforced by 3D entangled wires are shown in Figure 25. The wire segments show different morphologies in the matrix with homogeneous distribution. When the process is properly controlled, the introduction of wires has little influence on the microstructures of the matrix. In optimum conditions, the cohesion between the matrix and the wires is well obtained and no obvious traces of interface reaction can be observed because of the prevention of the reaction by the oxide barrier layer on the metallic wire [224], which offers the best improvement of the Young's modulus.

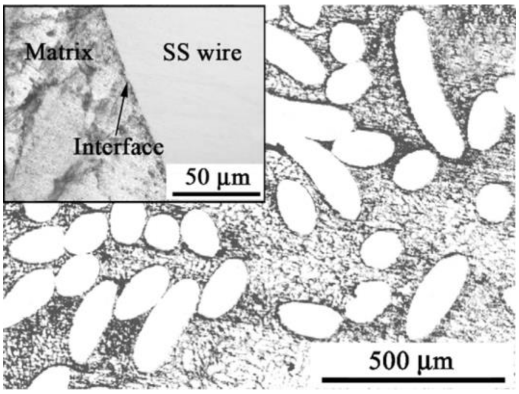

Figure 25. Microstructures of the A356 alloys reinforced by a preform with entangled 304 stainless steel wire at 17.7 vol.% [222].

The network structure of stainless steel can also be fabricated by sintering the wires before infiltrating the aluminium alloys through casting. The improvement of the Young's modulus without significantly scarifying the ductility is achievable in hybrid materials reinforced by an interconnected network of continuous wires of stainless steel [215]. Figure 26 shows the Young's modulus and the density of Al/steel cast hybrid materials versus the volume fraction of the interconnected network of continuous wires. It is obvious that the Young's modulus increases with increasing steel volume fraction. When the interconnected structures are used to improve the Young's modulus, the selection of the desirable volume fraction of the reinforcement and the structural design should be considered as important criteria.

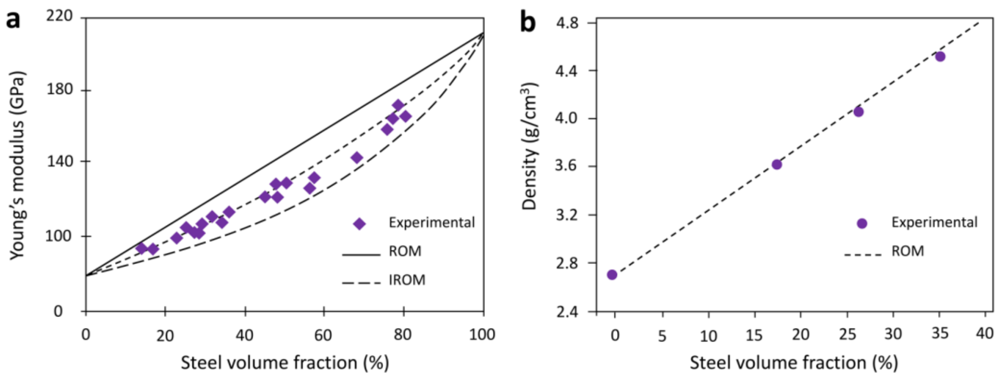

Figure 26. (a) Young's modulus and (b) density of Al-Si/steel cast hybrid materials with an interconnected network of continuous wires of stainless steel [215,216].

4.3 Al/iron hybrid materials

Interconnected wires in the form of three-dimensional preforms is an approach to improve the Young's modulus by continuous steel/iron reinforcement in Al alloys. Gupta et al. [225,226] fabricated several types of 3D preforms using the galvanised AISI 1008 wire of 0.8 mm diameter coated by 10.8 vol.% zinc. The geometries of the two types of reinforcement preforms are shown in Figure 27.

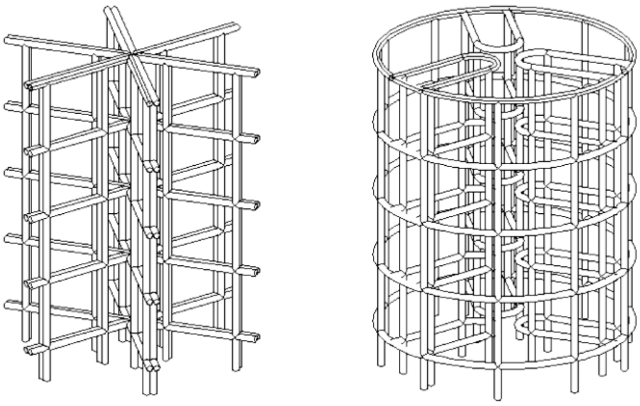

Figure 27. Schematic diagram of two different reinforcement preforms employed in Al/galvanised iron hybrid materials [225].

Table 16. Mechanical properties of aluminium reinforced with galvanised iron [227].

Materials	Young's modulus (GPa)	Yield strength (MPa)	Ultimate tensile strength (MPa)	Ductility (%)	Density (g/cm^3)	Specific stiffness GPa/g/cm^3)
Al (matrix)	70±2	101±6	120±3	17±9	2.7	25.9
Al/3vol.%Fe *	76±2	108±2	131±4	5±3	2.92	26.1
Al/3vol.%Fe *	81±2	152±4	186±15	5±4	2.81	28.8
Al/3vol.%Fe *	81±2	150±6	173±16	3±2	2.80	28.9
Al/5vol.%Fe	88±1	105±5	130±6	7±3	2.91	30.3

* With different wire arrangement.

The mechanical properties for the Al/Fe hybrid materials with AA1050 (99.5 wt.% Al) as the matrix are shown in Table 16. The incorporation of 3-5 vol.% of iron wires as reinforcement increases the Young's modulus, yield strength and ultimate tensile strength, but degrades the ductility. The Young's modulus is 88 GPa and the specific stiffness is 30.3 GPa/(g/cm^3) for the Al/5 vol.% Fe hybrid materials, which is much higher than that of the monolithic Al alloys. The measured Young's modulus of the hybrid Al/Fe materials exceeds the ROM prediction. This has been attributed to the combined effect of redistributing the fibre stress from the three-dimensional interconnected nature and the limited presence of the intermetallics at the interface [226]. Gupta et al. [228] fabricated aluminium-based hybrid materials containing titanium particles and iron mesh (continuous) reinforcement. Ti particles and the galvanised iron wire mesh (0.4 vol.% zinc and 0.8 mm wire diameter) are utilised as the continuous/interconnected reinforcement phase. The presence of hybrid reinforcement results in the 7.6% reduction in the coefficient of thermal expansion, the 10% increase in the Young's modulus, the 20% increase in the 0.2% yield strength and the 27% increase in the ultimate tensile strength.

As the critical characteristics in manufacturing the hybrid materials, the interface between steel/iron and aluminium has been extensively studied through different approaches due to the avoidance of formation of detrimental phases [229]. The interfaces between steel/iron and aluminium melt can be obtained by immersing the steel/iron into aluminium melt or overcasting aluminium melt onto the steel/iron surface. Dezellus et al. [230] studied the formation of the interface layer, by immersing mild steel into Al-Si alloy melts, and the mechanical properties of interface, by the pushout test. The results showed that the Al_5Fe_2Si and $Al_9Fe_2Si_2$ phases are formed at the interface and the crack initiation would occur in the intermetallic reaction layer. The formation of the intermetallic layer increases the mechanical properties of the hybrid materials.

Viala et al. [231] and Manasijevic et al. [232] prepared iron base insert reinforced Al-Si alloys by gravity casting and revealed that a continuous metallurgical bond at the iron insert/Al-Si alloy interface can be achieved via the formation of $FeAl_3$ and Fe_2Al_5 intermetallic phases on the interface. Bouayad et al. [233] found that several intermetallic compounds, including γ-Al_3FeSi, η-$Al_5Fe_2(Si)$ and β-Al_5FeSi, can be formed at the interface. The types of reaction products depend on the times and temperatures. Kobayashi and Yakou [234] reported that the common sequence to form the reaction layer is $Fe/Fe_2Al_5/FeAl_3/Al$, but Zhang et al. [235] showed that the sequence of the reaction layer is Fe/η-$Al_5Fe_2(Si)$/β-Al_5FeSi/Al–Si. The experimental results have confirmed that the surface modification of aluminising can promote the formation of sound surface and metallurgical bonding between steel and Al, which can be achieved by compound casting. Arghavani et al. [236] found that the Zn coating on the steel surface could enhance the wettability of bonding surface between steel and A5052 Al alloy. Liu et al. [237,238] found that the intermetallic compounds $Al_5Fe_2Zn_x$ and Al_3FeZn_x are formed at the interface between hot-dip galvanised steel and pure Al after compound casting. Generally, the Zincate must be at an appropriate thickness for the reaction during overcasting. If the thickness is more than the diffusion distance, the Zn layer will still exist in the final microstructure after overcasting, which is detrimental to the mechanical properties. This has been partially confirmed by Schwankl et al. [239] showing that the interface strength determined by zinc is the weakest part of the compound castings. If the coating is too thin, there are no sufficient compounds to provide bonding strength. Therefore, the bonding interface between the iron/steel and the aluminium alloy is the determining factor for manufacturing the hybrid materials.

4.4 Other hybrid materials

The Young's modulus of Al-based hybrid materials reinforced by other metals can be roughly estimated by the ROM model and the results are shown in Figure 28. Comparing with the Young's modulus of Fe and Ni at a level of ~200 GPa, the other continuous reinforcement – such as W and Mo

– have a higher potential for the improvement of stiffness. However, the cost and processing procedure will remain an issue in its application.

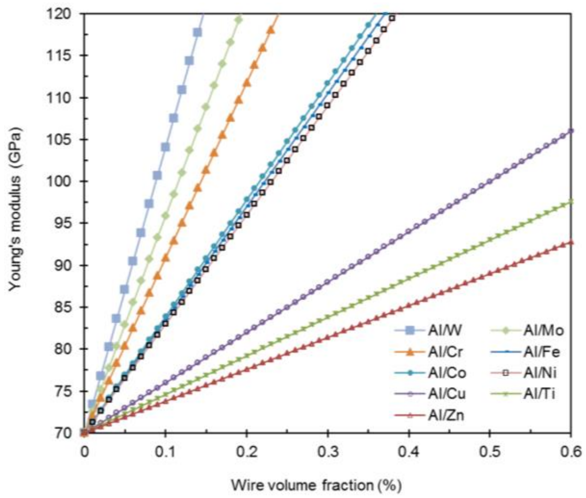

Figure 28. Young's modulus of aluminium-based hybrid materials reinforced with different types of metallic wires estimated by rule of mixtures.

5 Summary and future outlook

The Young's modulus of aluminium-based materials is one of the most important mechanical properties in controlling structural performance. The improvement of the Young's modulus of castable aluminium-based materials is essential for increasing their competiveness in light weighting structural applications. The capability of making complex shaped castings of these materials is critical in considering the massive production and the application in industry. The castability depends on the introduction methods, processing methods, volume fraction, size and distribution of the high modulus phases.

The influence of alloying elements on the Young's modulus depends on the state. If the alloying elements are in a solid solution phase, the magnitude of the Young's modulus is determined by the nature of the atomic interactions. If the alloying elements form second phases, the magnitude of the Young's modulus is determined by the volume fraction and the intrinsic modulus of the second phase. In Al alloys, the second phase is more effective for stiffness improvement than the solid solution. Among the available elements, Be, Li, Si, Cu, Mn and Ni are favourite candidates to enhance the modulus of cast aluminium alloys. However, Al-Li and Al-Be alloys are brittle, expensive and toxic, and there are difficulties in making shaped castings with complex geometry. Overall, the increase of Young's modulus in conventional cast aluminium alloys is usually less than 15% through adding alloying elements for manufacturing complex shaped castings. One of the major concerns is the reduction of the ductility of castings after adding specific elements to increase the Young's modulus. Therefore, further research into the improvement of Young's modulus and the ductility of aluminium alloys is necessary. Meanwhile, the existing intermetallic phases are not very effective at increasing Young's modulus. New intermetallic phases that can be formed through solidification are attractive for new alloys.

The improvement of the Young's modulus through introducing high modulus reinforcement phases as AMCs is an effective approach because of their high Young's modulus. The most capable reinforcement phases are TiB_2 (E=560 GPa) and SiC (E=480 GPa) for making shaped castings. Reinforcement phases can be added by ex-situ or in-situ methods, in which the in-situ method with particulate reinforcement is preferred for making castings with relatively complex shape and cavity. The main factors governing the Young's modulus of AMCs are the volume fraction, aspect ratio and the interface. The bonding between the matrix and the reinforcement is the most important factor in determining mechanical properties. Strong interfacial bonding provides effective load transfer from the matrix to the reinforcement for improved Young's modulus and other mechanical properties. The main concern on the performance of AMCs is their tendency to have relatively low ductility and fracture toughness when the materials provide high modulus. When using particulate-reinforced AMCs, the castability should be considered due to challenges in casting components with complex shape and cavity. The balance of castability/processibility and the improvement in Young's modulus is the key for further development.

Hybrid materials, made by metal wires with cast aluminium alloys, are effective for modulus improvement. In fact, hybrid materials can be considered a special type of composite material. The preforms made by continuous metallic wires as skeletons or frames are a key step. The pre-treatment of the surfaces are needed before casting. The overcasting can be any of the conventional casting methods. Knowledge in this area has not been well established for the variety of preform structures, pre-treatments and casting conditions; so continued study is necessary.

Stiff aluminium alloys are potentially one of the most promising materials for the significant reduction of structural weight with satisfied mechanical properties, including the Young's modulus. There are some knowledge gaps and challenges for the further development of high modulus cast aluminium alloys, which include:

a) The Young's modulus of aluminium alloys with multiple components are not fully understood. The development of complex Al-based alloys with the addition of desirable alloying elements is needed to ensure both high modulus and ductility properties.
b) Up to now, the main purpose for the addition of high modulus phase/reinforcement into the Al alloys has been to improve the wear resistance and high temperature performance. It is very important to carefully and specifically select the type as well as the volume fraction of reinforcement for modulus improvement.

c) Careful selection and combination of desirable alloying elements and in-situ formed reinforcement would possibly be the preferred option for developing the material with dominant stiffness properties, toughness and good castability.
d) In hybrid materials, reactivity between the reinforcement and the aluminium matrix must be carefully controlled to avoid the formation of brittle interface, which tends to lower the toughness of the interface. Hybrid materials can be considered for local stiffness improvement of the aluminium components.

References

[1] Miller WS, Zhuang L, Bottema J, et al. Recent development in aluminium alloys for the automotive industry. Mater Sci Eng A. 2000; 280(1):7-49.

[2] Dursun T, Soutis C. Recent developments in advanced aircraft aluminium alloys. Mater Des. 2014; 56: 862-871.

[3] Lloyd DJ. Particle reinforced aluminium and magnesium matrix composites. Int Mater Rev. 1994;39(1):1-23.

[4] Kaufman JG, Rooy EL. Aluminium alloy castings: properties, processes, and applications. ASM International; 2004.

[5] Bonnet F, Daeschler V, Petitgand G. High modulus steels: New requirement of automotive market. How to take up challenge? Can Metall Q. 2014;53:243-52.

[6] Zolotorevsky VS, Belov NA, Glazoff MV. Casting aluminium alloys. Oxford: Elsevier; 2007.

[7] Rohatgi PK. Metal matrix composites. Def Sci J. 2013;43(4):323-349.

[8] Mortensen A, Llorca J. Metal matrix composites. Annu Rev Mater Res. 2010;40:243-270.

[9] Bakshi SR, Lahiri D, Agarwal A. Carbon nanotube reinforced metal matrix composites-a review. Int Mater Rev. 2010;55:41-64.

[10] Kendig KL, Miracle DB. Strengthening mechanisms of an Al-Mg-Sc-Zr alloy, Acta Mater. 2002;50(16): 4165-4175.

[11] Li C, Chou TW. Elastic moduli of multi-walled carbon nanotubes and the effect of van der Waals forces. Compos Sci Technol. 2003;63:1517-1524.

[12] Gurtin ME. The linear theory of elasticity. Linear Theories of Elasticity and Thermoelasticity: Springer; 1973:1-295.

[13] Meyers MA, Chawla K.K. Mechanical behaviour of materials. vol. 2. Cambridge: Cambridge University Press, 2009.

[14] Masuda-Jindo K, Terakura K, Electronic theory for solid-solution hardening and softening of dilute Al based alloys: elastic-moduli enhancement of Al-Li alloys. Phys Rev B. 1989;39(11)7509.

[15] Wang WH. The elastic properties, elastic models and elastic perspectives of metallic glasses, Prog Mater Sci. 2012;57:487-656.

[16] Polmear I, StJohn D, Nie JF, et al. Light alloys: metallurgy of the light metals. Butterworth-Heinemann, 2017.

[17] Hull D, Clyne T. An introduction to composite materials: Cambridge University Press; 1996.

[18] Nieto A, Bisht A, Lahiri D, et al. Graphene reinforced metal and ceramic matrix composites: a review. Int Mater Rev. 2017;62:241-302.
[19] Tjong SC, Ma ZY. Microstructural and mechanical characteristics of in situ metal matrix composites. Mater Sci Eng R. 2000;29:149-113.
[20] Ibrahim I, Mohamed F, Lavernia E. Particulate reinforced metal matrix composites-a review. J Mater Sci. 1991;26:1137-1156.
[21] Lasagni F, Degischer HP. Enhanced young's modulus of Al-Si alloys and reinforced matrices by co-continuous structures. J Compos Mater. 2010;44:739-755.
[22] Standard AS. E8, Standard Test Methods for Tension Testing of Metallic Materials. Annual book of ASTM standards. 2004;3:57-72.
[23] ASTM E. 111-04: Standard test method for Young's modulus, tangent modulus, and chord modulus. Annual Book of ASTM Standards. 2004;3.
[24] ASTM C1419-99a. Standard test method for sonic velocity in refractory materials at room temperature and its use in obtaining an approximate Young's modulus. ASTM International, West Conshohocken, PA, 1999.
[25] Tefft W. Numerical solution of the frequency equations for the flexural vibration of cylindrical rods. J Res Natl Bur Stand B. 1960;64:237-42.
[26] ASTM E1876-01. Standard test method for dynamic young's modulus, shear modulus, and poisson's ratio by impulse excitation of vibration. American Society for Testing and Materials (ASTM), New York. 1876.
[27] ASTM E1875-13. Standard test method for dynamic Young's modulus, shear modulus, and Poisson's ratio by sonic resonance. Annual Book of ASTM Standards. 1875;3.
[28] Horst C, Saito T. Springer handbook of materials measurement methods. Ed. Leslie Smith. Vol. 32. Berlin: Springer, 2006.
[29] Smith JS, Wyrick MD, Poole JM. An evaluation of three techniques for determining the Young's modulus of mechanically alloyed materials. Dynamic elastic modulus measurements in materials 1990. ASTM International.
[30] Babicheva RI, et al. Elastic moduli of nanocrystalline binary Al alloys with Fe, Co, Ti, Mg and Pb alloying elements. Phil Mag. 2016;96:1598-1612.
[31] Mortensen A, Jin I. Solidification processing of metal matrix composites. Int Mater Rev. 1992:37(1):101-128.
[32] Kitabjian PH, Nix WD. Atomic size effects in Ni-Al based solid solutions. Acta Mater 1998;46(2):701-710.
[33] Uesugi T, Takigawa Y, Higashi K. Elastic constants of AlLi from first principles. Mater Trans. 2005;46(6): 1117-1121.
[34] Lubarda VA. On the effective lattice parameter of binary alloys. Mech Mater. 2003;35:53-68.
[35] Denton AR, Ashcroft NW, Vegard's law. Phys Rev A. 1991;43(6):3161.
[36] Noble B, Harris S, Dinsdale K. The elastic modulus of aluminium-lithium alloys. J Mater Sci. 1982;17(2):461-468.
[37] Eskin DG, Toropova L. Tensile and elastic properties of deformed heterogeneous aluminium alloys at room and elevated temperatures. Mater Sci Eng A. 1994;183(1):L1-L4.
[38] Jozwik P, Polkowski W, Bojar Z. Applications of Ni_3Al based intermetallic alloys-current stage and potential perceptivities. Materials. 2015;8(5):2537-2568.

[39] Tabibian S, et al. Influence of process-induced microstructure on hardness of two Al-Si alloys. Mater Sci Eng A. 2015;646:190-200.

[40] Meric C. An investigation on the elastic modulus and density of vacuum casted aluminium alloy 2024 containing lithium additions. J Mater Eng Perform. 2000;9(3):266-271.

[41] Rioja RJ, Fabrication methods to manufacture isotropic Al-Li alloys and products for space and aerospace applications. Mater Sci Eng A. 1998;257(1):100-107.

[42] Del Rio J, Plazaola F, Diego Nd. A positron annihilation study of the formation and dissolution of L12 precipitates in Al-Li alloys. Phil Mag A. 1994;69:591-6.

[43] Lavernia EJ, Srivatsan TS, Mohamed FA. Strength, deformation, fracture behaviour and ductility of aluminium-lithium alloys. J Mater Sci. 1990;25(2):1137-58.

[44] Prasad NE, Gokhale A, Wanhill R. Aluminium-Lithium alloys: processing, properties, and applications. 2013: Butterworth-Heinemann.

[45] Noble B, Harris S, Dinsdale K. Yield characteristics of aluminium–lithium alloys. Met Sci. 1982;16:425-30.

[46] Aftab-Alam D, Johnson D. Structural properties and relative stability of (meta)stable ordered, partially ordered, and disordered Al-Li alloy phases. Phys Rev B. 2012;85:1-8.

[47] Thompson G, Noble B. Precipitation characteristics of aluminium-lithium alloys containing magnesium. J Inst Met. 1973;101(4):111-115.

[48] Zhang SF, Zeng WD, Yang WH, et al. Ageing response of a Al-Cu-Li 2198 alloy. Mater Des. 2014;63:368-374.

[49] Romios M, Tiraschi R, Parrish C, et al. Design of multistep aging treatments of 2099 (C458) Al-Li Alloy. J Mater Eng Perform. 2005;14(5):641-646.

[50] Ott N, Kairy S, Yan K, et al. Evolution of grain boundary precipitates in an Al-Cu-Li alloy during aging. Metall Mater Trans A 2017;48(1):51-56.

[51] Noble B, Thompson G. Precipitation characteristics of aluminium-lithium alloys. Met Sci J. 1971;5(1):114-120.

[52] Sankaran K, Grant N. The structure and properties of splat-quenched aluminium alloy 2024 containing lithium additions. Mater Sci Eng. 1980;44(2):213-227.

[53] Samuel FH, Champier G. Microstructural characterization of centrifugally atomized Al-Li-X powders: Effect of Si and Co additions. In Production, Refining, Fabrication and Recycling of Light Metals, Proceedings of the International Symposium on Production, Refining, Fabrication and Recycling of Light Metals, Hamilton, Ontario, August 26-30, 1990, p.287-297.

[54] Fox AG, Fisher RM. The origin of the high elastic modulus in Al-Li alloys. J Mater Sci Lett. 1988;7(3):301-303.

[55] Lendvai J. Precipitation and strengthening in aluminium alloys. Mater Sci Forum. 1996;217: 43-56.

[56] Totten GE, MacKenzie DS, editors. Handbook of aluminum: Vol. 1: physical metallurgy and processes. CRC Press; 2003.

[57] Quist WE, Narayanan GH. Aluminum-lithium alloys. aluminum alloys-contemporary research and applications. 2012;31:219-254.

[58] Rioja RJ, Liu J. The evolution of Al-Li base products for aerospace and space applications. Metall and Mater Trans A. 2012;43(9):3325-3337.
[59] Fridlyander I. High-modulus aluminium alloys with beryllium and magnesium. Met Sci Heat Treat. 2003;45(9):348-350.
[60] Marder JM, Haws WJ. Semi-solid processing of beryllium-containing alloys of magnesium. US5679182 A (Application number US 08/313,994).
[61] Walsh KA. Beryllium chemistry and processing. 2009: ASM International.
[62] Speer W, Es-Said OS. Applications of an aluminium–beryllium composite for structural aerospace components. Eng Fail Anal. 2004;11(6):895-902.
[63] Bowden D, et al. Characterization of aluminium-beryllium alloy sheet. Mater Sci Forum. 2000;331-337:901-906.
[64] Grensing FC, Marder JM, Brophy JH. Aluminium alloys containing beryllium and investment casting of such alloys. 1997, US5667600 A (Application number US 08/221,395).
[65] Marder JM, Haws WJ, Beryllium-containing alloys of aluminium and semi-solid processing of such alloys. 1998, CA2161252 A1 (Application number CA 2161252).
[66] Parsonage TB. Development of aluminium beryllium for structural applications. Adv Mater Opt Prec Struc 1997;1:236-248.
[67] Nekrasova G, Yatsenko K, New light high-modulus beryllium-aluminium alloys of the lockalloy type for space vehicles. Met Sci Heat Treat. 1965;7(6):411-413.
[68] Nieh TG, Henshall CA, Wadsworth J. High-temperature properties of rapidly solidified Al-Be alloys. J Mater Sci. 1987;22:4411-4416
[69] Crooks DD, Fenn RWJ, Mccarthy WH. Ternary, quaternary and more complex alloys of Be-Al. 1972, US3664889 A.
[70] Jones CR, Krock RH, Larsen EI. Beryllium-aluminium-silver composite. 1967, US3373002 A.
[71] Jones CR, Krock RH, Larsen EI. Composites of beryllium-aluminium-zinc. 1967, US3379513 A.
[72] Jones CR, Krock RH, Larsen EI. Beryllium-aluminium-silicon composite. 1969, US3438751 A.
[73] Ochiai T, Yamada H, Hoshi M. Aluminium-beryllium-silicon based alloy. 2003, US6656421 B2 (US 09/974,752).
[74] Speer W, Es-Said OS. Applications of an aluminium-beryllium composite for structural aerospace components. Eng Fail Anal. 2004;11(6):895-902.
[75] Levoy NF, Nachtrab WT, Raftery KR. Light-weight, high strength beryllium-aluminium alloy. 1994, EP0670912 B1 (EP19940927322).
[76] ASM handbook. 2. Properties and selection: nonferrous alloys and special-purpose materials. 2009: ASM International.
[77] Hegde S, Prabhu KN. Modification of eutectic silicon in Al-Si alloys. J Mater Sci. 2008;43(9):3009-3027.
[78] Timpel M, et al. The role of strontium in modifying aluminium-silicon alloys. Acta Mater. 2012;60(9):3920-3928.
[79] Nikanorov SP, Volkov MP, Gurin VN, et al. Structural and mechanical properties of Al–Si alloys obtained by fast cooling of a levitated melt. Mater Sci Eng A. 2005; 390(1):63-69.
[80] Warmuzek M. Aluminium-silicon casting alloys: An atlas of microfractographs. 2004: ASM International.

[81] Lasagni F, Degischer HP. Enhanced Young's modulus of Al-Si alloys and reinforced matrices by co-continuous structures. J Compos Mater. 2010;44(6):739-755.
[82] Polmear I, John DS. Light alloys: From traditional alloys to nanocrystals. 2005: Butterworth-Heinemann.
[83] Lasagni F, Lasagni A, Marks E, et al. Three-dimensional characterization of as-cast and solution-treated AlSi12 (Sr) alloys by high-resolution FIB tomography. Acta Mater. 2007;55(11):3875-3882.
[84] Radutoiu N, Alexis J, Lacroix L, et al. Effect of the over-ageing treatment on the mechanical properties of AA2024 aluminium alloy. Revista De Chimie. 2012;63:1042-1045.
[85] Jeong CY. Effect of alloying elements on high temperature mechanical properties for piston alloy. Mater Trans. 2012;53(1):234-239.
[86] Hussey RJ, Wilson J. Light alloys: Directory and databook. 2013: Springer Science & Business Media.
[87] Caceres C, et al. The effect of Cu content on the level of microporosity in Al-Si-Cu-Mg casting alloys. Scripta Mater. 1999;40(5):631-637.
[88] Li Z, et al. Effect of alloying elements on the segregation and dissolution of $CuAl_2$ phase in Al-Si-Cu 319 alloys. J Mater Sci. 2003;38(6):1203-1218.
[89] Djurdjevic M, Stockwell T, Sokolowski J. The effect of strontium on the microstructure of the aluminium-silicon and aluminium-copper eutectics in the 319 aluminium alloy. Inter J Cast Met Res. 1999;12(2):67-73.
[90] Abo-Elsoud M, Esmail H, Sobhy M. Correlation between elastic modulus of Al–Cu alloys and metallurgical characteristics of their constituent elements. Radiat Eff Defects Solids. 2007;162(9):685-690.
[91] Dudzinski N. The Young's modulus, Poisson's ratio, and rigidity modulus of some aluminium alloys. J. Inst Met. 1952;81.
[92] Fouquet F, et al. Variation du module d'young associee a la precipitation de la phase θ′ dans un alliage Al-Cu 4%. Acta Metall. 1979;27(3):315-326.
[93] Samuel A, Gauthier J, Samuel F. Microstructural aspects of the dissolution and melting of Al_2Cu phase in Al-Si alloys during solution heat treatment. Metall Mater Trans A. 1996;27(7):1785-1798.
[94] Gao Y, et al. Atomic bonding and properties of Al-Cu alloy with ϑ (Al_2Cu). J Electronic Mater. 2006;35(10):1801-1805.
[95] Peters M, Bunk W. Low density, high-stiffness, aluminium-lithium materials. J Aircraft. 1990;27(5):456-458.
[96] Hafez HA, Farag MM. Effect of structure on the Young's modulus of Al-Cu-Ni alloys. J Mater Sci. 1981;16(5):1223-1232.
[97] Lasa L, Rodriguez-Ibabe J. Characterization of the dissolution of the Al_2Cu phase in two Al-Si-Cu-Mg casting alloys using calorimetry. Mater Character. 2002;48(5):371-378.
[98] Kaufman JG. Properties of aluminium alloys: tensile, creep, and fatigue data at high and low temperatures. ASM international; 1999.

[99] Grabel JV, Cost JR. Ultrasonic velocity measurement of elastic constants of Al-Al_3Ni unidirectionally solidified eutectic. Metall Trans. 1972;3(7):1973-1978.
[100] McConnell M, Partridge P. The effect of microstructure and composition on the properties of vapour quenched Al-Cr alloys–I. Young's modulus. Acta Metall. 1987;35(8):1973-1980.

[101] Partridge P, McConnell M. The effect of microstructure and composition on the properties of vapour quenched Al-Cr alloys–II. Tensile properties. Acta Metall. 1987;35(8):1981-1993.

[102] Zhang J, et al. Microstructural development of Al-15wt.% Mg_2Si in situ composite with mischmetal addition. Mater Sci Eng A. 2000;281(1):104-112.

[103] Qin Q, et al. Semisolid microstructure of Mg_2Si/Al composite by cooling slope cast and its evolution during partial remelting process. Mater Sci Eng A. 2007;444(1):99-103.

[104] Ramnath BV, Elanchezhian C, Annamalai1 RM, et al. Aluminium metal matrix composites – a review. Rev Adv Mater Sci. 2014;38:55-60.

[105] Tian K, et al. Effects of in situ generated ZrB_2 nano-particles on microstructure and tensile properties of 2024Al matrix composites. J Alloys Comp. 2014;594:1-6.

[106] Ibrahim IA, Mohamed FA, Lavernia EJ. Particulate reinforced metal matrix composites-a review. J Mater Sci. 1991;26(5):1137-1156.

[107] Kainer KU, Basics of metal matrix composites in book: Metal matrix composites: Custom-made materials for automotive and aerospace engineering. 2006;1-54.

[108] Chawla KK. Metal matrix composites: Wiley Online Library; 2006.

[109] Mathew J, Mandal A, Kumar SD. Effect of semi-solid forging on microstructure and mechanical properties of in-situ cast Al-Cu-TiB_2 composites. J Alloys Comp. 2017;712:460-467.

[110] Fan Z, Wang Y, Zhang Y, et al. Grain refining mechanism in the Al/Al-Ti-B system. Acta Mater. 2015;84:292-304.

[111] Aghajanian MK, Rocazella MA, Burke JT, et al. The fabrication of metal matrix composites by a pressureless infiltration technique. J Mater Sci. 1991;26(2):447-454.

[112] Prasad SV, Asthana R. Aluminium metal-matrix composites for automotive applications: Tribological considerations. Tribol Lett. 2004;17(3):445-453.

[113] Amirkhanlou S, Niroumand B. Development of Al356/SiC_p cast composites by injection of SiC_p containing composite powders. Mater Des. 2011;32(4):1895-1902.

[114] Amirkhanlou S, Niroumand B. Effects of reinforcement distribution on low and high temperature tensile properties of Al356/SiC_p cast composites produced by a novel reinforcement dispersion technique. Materi Sci Eng A. 2011;528(24):7186-7195.

[115] Jacobson LA, McKittrick J. Rapid solidification processing. Mater Sci Eng R. 1994;11(8):355-408.

[116] Asta M, Beckermann C, Karma A. Solidification microstructures and solid-state parallels: Recent developments, future directions. Acta Mater. 2009;57(4):941-971.

[117] Sree Manu KM, Arun Kumar S, Rajan TPD, et al. Effect of alumina nanoparticle on strengthening of Al-Si alloy through dendrite refinement, interfacial bonding and dislocation bowing. J Alloys Comp. 2017;712:394-405.

[118] Ted Guo ML, et al. Tribological behaviour of aluminium/SiC/nickel-coated graphite hybrid composites. Mater Sci Eng A. 2002;333:134-145.

[119] Rohatgi PK, Pasciak K, Narendranath CS, et al. Evolution of microstructure and local thermal conditions during directional solidification of A356-SiC particle composites. J Mater Sci. 1994;29(20):5357-5366.

[120] Zhao D, Tuler FR, Lloyd DJ. Fracture at elevated temperatures in a particle reinforced composite. Acta Metall Mater. 1994;42(7):2525-2533.

[121] Asghar Z, Requena G, Boller E. Three-dimensional rigid multiphase networks providing high-temperature strength to cast AlSi10Cu5Ni1-2 piston alloys. Acta Mater. 2011;59(16):6420-6432.

[122] Springer H, Aparicio Fernandez R, Duarte MJ, et al. Microstructure refinement for high modulus in-situ metal matrix composite steels via controlled solidification of the system Fe-TiB2. Acta Mater. 2015;96:47-56.

[123] Zhang H, Springer H, Aparicio-Fernandez R, et al. Improving the mechanical properties of Fe-TiB_2 high modulus steels through controlled solidification processes. Acta Mater. 2016;118:187-195.

[124] Gao Q, et al. Improvement of particles distribution of in-situ 5 vol% TiB_2 particulates reinforced Al-4.5 Cu alloy matrix composites with ultrasonic vibration treatment. J Alloys Comp. 2017;692:1-9.

[125] Gao Q, et al. Preparation of in-situ 5vol% TiB_2 particulate reinforced Al-4.5 Cu alloy matrix composites assisted by improved mechanical stirring process. Mater Des. 2016;94:79-86.

[126] Zhang J, Fan Z. Microstructure and mechanical properties of in situ Al-Mg_2Si composites. Mater Sci Technol. 2000;16(7-8):913-918.

[127] Basu B, Balani K. Advanced structural ceramics. 2011: John Wiley & Sons.

[128] Kainer KU, editor. Metal matrix composites: custom-made materials for automotive and aerospace engineering. John Wiley & Sons; 2006 Aug 21.

[129] Liu GR. A step-by-step method of rule-of-mixture of fiber-and particle-reinforced composite materials. Compos Struct. 1997;40:313-322.

[130] Halpin JC, Kardos JL. The Halpin-Tsai equations: A review. Polymer Eng Sci. 1976;16:344-352.

[131] Hashin Z, Shtrjkman S. A variational approach to the theory of the elastic behaviour of multiphase materials. J Mech Phys Solids. 1963;11:127-140.

[132] Tuchinskii L. Elastic constants of pseudoalloys with a skeletal structure. Powder Metall Met Ceram. 1983;22:588-95.

[133] Hull D, Clyne T. An introduction to composite materials: Cambridge University Press; 1996.

[134] Peng H. A review of consolidation effects on tensile properties of an elemental Al matrix composite. Mater Sci Eng A. 2005;396:1-2.

[135] Liu Z, et al. Effect of ultrasonic vibration on microstructural evolution of the reinforcements and degassing of in situ TiB_{2p}/Al-12Si-4Cu composites. J Mater Process Technol. 2012;212(2):365-371.

[136] Geng J, et al. The solution treatment of in-situ sub-micron TiB_2/2024 Al composite. Mater Des. 2016;98:186-193.

[137] Hong T, Shen Y, Geng J, et al. Effect of cryogenic pre-treatment on aging behavior of in-situ TiB_2/Al–Cu–Mg composites. Mater Charac. 2016; 119:40-46.

[138] Tee K, Lu L, Lai M. In situ stir cast Al-TiB_2 composite: Processing and mechanical properties. Mater Sci Technol. 2001;17(2):201-206.

[139] Tee KL, Lu L, Lai M. In situ processing of Al-TiB_2 composite by the stir-casting technique. J Mater Process Technol. 1999;89:513-519.

[140] Tee K, Lu L, Lai M. Synthesis of in situ Al-TiB_2 composites using stir cast route. Compos Struct. 1999;47(1):589-593.

[141] Changizi A, Kalkanli A, Sevinc N. Production of in situ aluminium–titanium diboride master alloy formed by slag–metal reaction. J Alloys Comp. 2011;509(2):237-240.

[142] Lü L, et al. In situ TiB_2 reinforced Al alloy composites. Scripta Mater. 2001;45(9):1017-1023.

[143] Mathew J, et al. X-ray tomography studies on porosity and particle size distribution in cast in-situ Al-Cu-TiB_2 semi-solid forged composites. Mater Charact. 2016;118:57-64.
[144] Mandal A, Chakraborty M, Murty B. Ageing behaviour of A356 alloy reinforced with in-situ formed TiB_2 particles. Mater Sci Eng A, 2008;489(1):220-226.
[145] Tee K, Lu L, Lai M. In situ stir cast Al-TiB_2 composite: Processing and mechanical properties. Mater Sci Technol. 2001;17(2):201-206.
[146] Feng C, Froyen L. Microstructures of in situ Al/TiB_2 MMCs prepared by a casting route. J Mater Sci. 2000;35(4):837-850.
[147] Chen XH, Yan H. Solid–liquid interface dynamics during solidification of Al 7075-Al_2O_{3np} based metal matrix composites. Mater Des. 2016 Mar 15;94:148-58.
[148] Chen Z, et al. Development of TiB_2 reinforced aluminium foundry alloy based in situ composites – Part I: An improved halide salt route to fabricate Al-5wt% TiB2 master composite. Mater Sci Eng A. 2014;605:301-309.
[149] Mandal A, Murty B, Chakraborty M. Sliding wear behaviour of T6 treated A356-TiB_2 in-situ composites. Wear. 2009;266(7):865-872.
[150] Amirkhanlou S, Ji S, Zhang Y, et al. High modulus Al-Si-Mg-Cu/Mg_2Si-TiB_2 hybrid nanocomposite: Microstructural characteristics and micromechanics-based analysis. J Alloy Compd. 2017;694:313-324.
[151] Westwood A. Materials for advanced studies and devices. Metall Trans A. 1988;19(4):749-758.
[152] Li G, Zheng M, Chen G. Mechanism and kinetic model of in-situ TiB_2/7055Al nanocomposites synthesized under high intensity ultrasonic field. J Wuhan Uni Technol Mater Sci Ed. 2011;26(5):920-925.
[153] Kumar S, et al. Tensile and wear behaviour of in situ Al-7Si/TiB_2 particulate composites. Wear. 2008; 265(1):134-142.
[154] Han G, et al. High-temperature mechanical properties and fracture mechanisms of Al-Si piston alloy reinforced with in situ TiB_2 particles. Mater Sci Eng A. 2015;633:161-168.
[155] Lü L, et al. In situ TiB_2 reinforced Al alloy composites. Scripta Mater. 2001;45(9):1017-1023.
[156] Kumar S, Sarma VS, Murty B. Effect of temperature on the wear behaviour of Al-7Si-TiB_2 in-situ composites. Metall Mater Trans A. 2009;40(1):223-231.
[157] Wang M, et al. Mechanical properties of in-situ TiB_2/A356 composites. Mater Sci Eng A. 2014;590:246-254.
[158] Chang R, Graham LJ. Low-temperature elastic properties of ZrC and TiC. J Applied Phys. 1966;37(10):3778-3783.
[159] Jiang W, et al. Synthesis of TiC/Al composites in liquid aluminium. Mater Lett. 1997;32(2):63-65.
[160] Lijay KJ, et al. Microstructure and mechanical properties characterization of AA6061/TiC aluminium matrix composites synthesized by in situ reaction of silicon carbide and potassium fluotitanate. Trans Nonferr Met Soc China. 2016;26(7):1791-1800.
[161] Liang Y, Zhou J, Dong S. Microstructure and tensile properties of in situ TiC_p/Al-4.5 wt.% Cu composites obtained by direct reaction synthesis. Mater Sci Eng A. 2010;527(29):7955-7960.
[162] Liu Z, et al. Synthesis of submicrometer-sized TiC particles in aluminium melt at low melting temperature. J Mater Res. 2014;29(7):896-901.

[163] Li P, Kandalova E, Nikitin V. In situ synthesis of Al-TiC in aluminium melt. Mater Lett. 2005;59(19):2545-2548.
[164] Tyagi R. Synthesis and tribological characterization of in situ cast Al-TiC composites. Wear. 2005;259(1): 569-576.
[165] Yang B, Chen G, Zhang J. Effect of Ti/C additions on the formation of Al_3Ti of in situ TiC/Al composites. Mater Des. 2001;22(8):645-650.
[166] Samer N, et al. Microstructure and mechanical properties of an Al-TiC metal matrix composite obtained by reactive synthesis. Composites Part A. 2015;72:50-57.
[167] Mohapatra S, et al. Fabrication of Al-TiC composites by hot consolidation technique: Its microstructure and mechanical properties. J Mater Res Technol. 2016;5(2):117-122.
[168] Amosov AP, Luts A, Ermoshkin A. Nanostructured aluminium matrix composites of Al-10% TiC obtained in situ by the SHS method in the melt. Key Eng Mater. 2016;684:281-286.
[169] Hashin Z, Shtrikman S. A variational approach to the elastic behaviour of multiphase materials: J Mech Phys Solid. 1962;11:127-140.
[170] Tong X, Fang H. Al-TiC composites in situ-processed by ingot metallurgy and rapid solidification technology: Part II. Mechanical behaviour. Metall Mater Trans A. 1998;29(3):893-902.
[171] Kumar A, Jha P, Mahapatra M. Abrasive wear behaviour of in Situ TiC reinforced with Al-4.5% Cu matrix. J Mater Eng Perform. 2014;23(3):743-752.
[172] Lee JC, Byun JY, Park SB, et al. Prediction of Si contents to suppress the formation of Al_4C_3 in the SiC_p/Al composite. Acta Mater. 1998;46(5):1771-1780.
[173] Peng Z, Fuguo L. Effects of particle clustering on the flow behaviour of SiC particle reinforced Al metal matrix composites. Rare Met Mater Eng. 2010;39(9):1525-1531.
[174] Balasivanandha Prabhu S, Karunamoorthy L, Kathiresan S, et al. Influence of stirring speed and stirring time on distribution of particles in cast metal matrix composite. Mater Process Technol. 2006;171:268-273.
[175] Tzamtzis S, Barekar NS, Hari Babu N, et al. Processing of advanced Al/SiC particulate metal matrix composites under intensive shearing-A novel Rheo-process. Composites Part A. 2009;40:144-151.
[176] Properties AH. Selection: Nonferrous alloys and special-purpose materials, vol. 2. ASM International, Materials, Park, OH, 1990.
[177] Kumar BA, Murugan N. Metallurgical and mechanical characterization of stir cast AA6061-T6–AlN_p composite. Mater Des. 2012;40:52-8.
[178] Yu P, et al. In situ fabrication and mechanical properties of Al-AlN composite by hot extrusion of partially nitrided AA6061 powder. J Mater Res. 2011;26(14):1719-1725.
[179] Yang C, et al. Microstructure and mechanical properties of AlN particles in situ reinforced Mg matrix composites. Mater Sci Eng A. 2016;674:158-163.
[180] Hou Q, Mutharasan R, Koczak M. Feasibility of aluminium nitride formation in aluminium alloys. Mater Sci Eng A. 1995;195:121-129.
[181] Zheng Q, Reddy R. Mechanism of in situ formation of AlN in Al melt using nitrogen gas. J Mater Sci. 2004;39(1):141-149.
[182] Kumari SS, Pillai U, Pai B. Synthesis and characterization of in situ Al-AlN composite by nitrogen gas bubbling method. J Alloy Compd. 2011;509(5):2503-2509.

[183] Zheng Q, Reddy RG. Kinetics of in-situ formation of AlN in Al alloy melts by bubbling ammonia gas. Metall Mater Trans B. 2003;34(6):793-804.

[184] Chedru M, Chermant JL, Vicens J. Thermal properties and Young's modulus of Al-AlN composites. J Mater Sci Lett. 2001;20:893-895.

[185] Balog M, Krizik P, Yan M, et al. SAP-like ultrafine-grained Al composites dispersion strengthened with nanometric AlN. Mater Sci Eng A. 2013;588:181-187.

[186] Dinaharan I, Murugan N, Parameswaran S. Influence of in situ formed ZrB_2 particles on microstructure and mechanical properties of AA6061 metal matrix composites. Mater Sci Eng A. 2011;528(18):5733-5740.

[187] Zhang SL, et al. Fabrication and dry sliding wear behaviour of in situ Al-K_2ZrF_6-KBF_4 composites reinforced by Al_3Zr and ZrB_2 particles. J Alloy Compd. 2008;450(1):185-192.

[188] Zhao Y, et al. Effects of molten temperature on the morphologies of in situ Al_3Zr and ZrB_2 particles and wear properties of (Al_3Zr+ZrB_2)/Al composites. Mater Sci Eng A. 2007;457(1):156-161.

[189] Zhao D, et al. In-situ preparation of Al matrix composites reinforced by TiB_2 particles and sub-micron ZrB_2. J Mater Sci. 2005;40(16):4365-4368.

[190] Rengasamy N, Rajkumar M, Kumaran SS. An analysis of mechanical properties and optimization of EDM process parameters of Al 4032 alloy reinforced with ZrB_2 and TiB_2 in-situ composites. J Alloy Compd. 2016;662:325-338.

[191] Mahamani A, et al. Synthesis, quantitative elemental analysis, microstructure characteristics and micro hardness analysis of AA2219 aluminium alloy matrix composite reinforced by in-situ TiB_2 and sub-micron ZrB_2 particles. Frontiers Auto Mech Eng (FAME). 2010;25:50-53.

[192] Dinaharan I, Murugan N. Dry sliding wear behaviour of AA6061/ZrB_2 in-situ composite. Trans Nonferr Met Soci China. 2012;22(4):810-818.

[193] Kumar GN, et al. Dry sliding wear behaviour of AA 6351-ZrB_2 in situ composite at room temperature. Mater Des. 2010;31(3):1526-1532.

[194] Selvam JDR, Dinaharan I. In situ formation of ZrB_2 particulates and their influence on microstructure and tensile behaviour of AA7075 aluminium matrix composites. Eng Sci Technol Inter J. 2017;20(1):187-196.

[195] Gautam G, et al. High temperature tensile and tribological behaviour of hybrid (ZrB_2+Al_3Zr)/AA5052 in situ composite. Metall Mater Trans A. 2016;47(9):4709-4720.

[196] Gautam G, Mohan A. Effect of ZrB_2 particles on the microstructure and mechanical properties of hybrid (ZrB_2+Al_3Zr)/AA5052 in situ composites. J Alloy Compd. 2015;649:174-183.

[197] Wang K, et al. Fabrication of in situ AlN-TiN/Al inoculant and its refining efficiency and reinforcing effect on pure aluminium. J Alloy Compd. 2013;547:5-10.

[198] Zhang Y, Ma N, Wang H. Improvement of yield strength of LM24 alloy. Mater Des. 2014;54:14-17.

[199] Rohatgi P, Asthana R, Das S. Solidification, structures, and properties of cast metal-ceramic particle composites. Inter Met Rev. 1986;31(1):115-139.

[200] Amirkhanlou S, Rezaei MR, Niroumand B, Toroghinejad MR. High-strength and highly-uniform composites produced by compocasting and cold rolling processes. Mater Des. 2011;32:2085-2090.

[201] Lee PD, Hunt JD. Hydrogen porosity in directional solidified aluminium-copper alloys: in situ observation. Acta Mater. 1997;45(10):4155-4169.

[202] Villuendas A, Jorba J, Roca A. The role of precipitates in the behaviour of Young's modulus in aluminium alloys. Metall Mater Trans A. 2014;45(9):3857-3865.
[203] Aghajanian MK, Burke J, White DR, et al. A new infiltration process for the fabrication of metal matrix composites. Sampe Quarterly. 1989;20:43-46.
[204] Aghajanian MK, Rocazella MA, Burke JT, et al. The fabrication of metal matrix composites by a pressureless infiltration technique. J Mater Sci. 1991;26:447-454.
[205] Chen J, Hao C, Zhang J. Fabrication of 3D-SiC network reinforced aluminium-matrix composites by pressureless infiltration. Mater Lett. 2006;60:2489-2492.
[206] Daehn GS, Starck B, Xu L. Elastic and plastic behaviour of a co-continuous alumina/aluminium composite. Acta Mater. 1996;44:249-261.
[207] Clyne T, Mason J. The squeeze infiltration process for fabrication of metal-matrix composites. Metall Trans A. 1987;18(8):1519-1530.
[208] Acilar M, Gul F. Effect of the applied load, sliding distance and oxidation on the dry sliding wear behaviour of Al–10Si/SiCp composites produced by vacuum infiltration technique. Mater Des. 2004;25(3):209-217.
[209] Xie XL, Mai YW, Zhou XP. Dispersion and alignment of carbon nanotubes in polymer matrix: A review. Mater Sci Eng R. 2005;49:89-112.
[210] Porwal H, Grasso S, Reece MJ. Review of graphene-ceramic matrix composites. Adv. Appl. Ceram. 2013;112(8): 443-454.
[211] Zhang X, Chen W, Luo H, et al. Formation of periodic layered structure between novel Fe-Cr-B cast steel and molten aluminium. Scripta Mate. 2017;130:288-291.
[212] Nair SV, Tien JK, Bates RC. Sic-reinforced aluminium metal matrix composites. Inter Met Rev. 1985;30(1):275-290.
[213] Christman T, Suresh S. Microstructural development in an aluminium alloy-SiC whisker composite. Acta Metall. 1988;36(7):1691-1704.
[214] Rohatgi PK, Asthana R, Das S. Solidification, structures, and properties of cast metal-ceramic particle composites. Inter Met Rev. 1986;31(1):115-139.
[215] Boland F, et al. Tensile flow properties of Al-based matrix composites reinforced with a random planar network of continuous metallic fibres. Acta Mater. 1998;46(18):6311-6323.
[216] Ryelandt L, Salmon C, Delannay F. Neutron diffraction analysis of the evolution of phase stresses during plastic straining of aluminium matrix composites reinforced with a continuous, random planar network of fibres. Mater Sci Forum. 2000;347-349:486-491.
[217] Salmon C, et al. Mechanical properties of aluminium/Inconel 601 composite wires formed by swaging. J Mater Sci. 1998;33(23):5509-5516.
[218] Villuendas A, Jorba J, Roca A. The role of precipitates in the behaviour of Young's modulus in aluminium alloys. Metall Mater Trans A. 2014;45(9):3857-3865.
[219] Salmon C, et al. Influence of the oxidation conditions of the fibres on the mechanical properties of Al matrix composites reinforced with Ni-based fibres. Mater Sci Forum. 2001; 369-372: 435-442.
[220] Salmon C, et al. Strengthening of Al/Ni-based composites by in situ growth of intermetallic particles. Mater Sci Eng A. 2002;334(1):193-200.

[221] Boland F, Colin C, Delannay F. Control of interfacial reactions during liquid phase processing of aluminium matrix composites reinforced with INCONEL 601 fibers. Metall Mater Trans A. 1998;29(6):1727-1739.

[222] Tan Q, He G. 3D entangled wire reinforced metallic composites. Mater Sci Eng A. 2012;546:233-238.

[223] Tan Q, et al. Mechanical behaviours of quasi-ordered entangled aluminium alloy wire material. Mater Sci Eng A. 2009;527(1-2):38-44.

[224] Guler K, Kisasoz A, Karaaslan A. Investigation of Al/Steel bimetal composite fabrication by vacuum assisted solid mould investment casting. Acta Phys Polonica A. 2014;126(6):1327-1330.

[225] Ganesh V, Lee C, Gupta M. Enhancing the tensile modulus and strength of an aluminium alloy using interconnected reinforcement methodology. Mater Sci Eng A. 2002;333(1):193-198.

[226] Gupta M, Lai MO, Lim CYH. Development of a novel hybrid aluminium-based composite with enhanced properties. J Mater Process Technol. 2006;176(1-3):191-199.

[227] Ganesh V, Gupta M. Effect of the extent of reinforcement interconnectivity on the properties of an aluminium alloy. Scripta Mater. 2001;44(2):305-310.

[228] Gupta M, Lai M, Lim C. Development of a novel hybrid aluminium-based composite with enhanced properties. J Mater Process Technol. 2006;176(1):191-199.

[229] Haddadi F. Microstructure reaction control of dissimilar automotive aluminium to galvanized steel sheets ultrasonic spot welding. Mater Sci Eng A. 2016;678:72-84.

[230] Dezellus O, Digonnet B, Sacerdote-Peronnet M, et al. Mechanical testing of steel/aluminium-silicon interfaces by pushout. Int. J. Adhes. 2007;27:417-421.

[231] Viala J, Peronnet M, Barbeau F, et al. Interface chemistry in aluminium alloy castings reinforced with iron base inserts. Compos Part A. 2002;33:1417-1420.

[232] Manasijevic S, Radiša R, Brodarac ZZ, et al. 2015. Al-Fin bond in aluminium piston alloy & austenitic cast iron insert. Int. J. Met. 2015;9:27-32.

[233] Bouayad A, Gerometta C, Belkebir A, et al. Kinetic interactions between solid iron and molten aluminium. Mater Sci Eng A. 2003;363:53-61.

[234] Kobayashi S, Yakou T. Control of intermetallic compound layers at interface between steel and aluminium by diffusion-treatment. Mater Sci Eng A. 2002;338:44-53.

[235] Zhang K, Bian X, Li Y, et al. New evidence for the formation and growth mechanism of the intermetallic phase formed at the Al/Fe interface. J Mater Res. 2013;95:3279-3287.

[236] Arghavani MR, Movahedi M, Kokabi AH. Role of zinc layer in resistance spot welding of aluminium to steel. Mater Des. 2016;102:106-114.

[237] Liu Y, Bian X, Zhang K, et al. Interfacial microstructures and properties of aluminium alloys/galvanized low-carbon steel under high-pressure torsion. Mater Des. 2014;64:287-293.

[238] Liu T, Wang Q, Sui Y, et al. An investigation into aluminium–aluminium bimetal fabrication by squeeze casting. Mater Des. 2015;68:8-17.

[239] Schwankl M, Wedler J, Körner C. Wrought Al-Cast Al compound casting based on zincate treatment for aluminium wrought alloy inserts. J Mater Process Technol. 2016;238:160-168.